CHALMERS
UNIVERSITY OF TECHNOLOGY

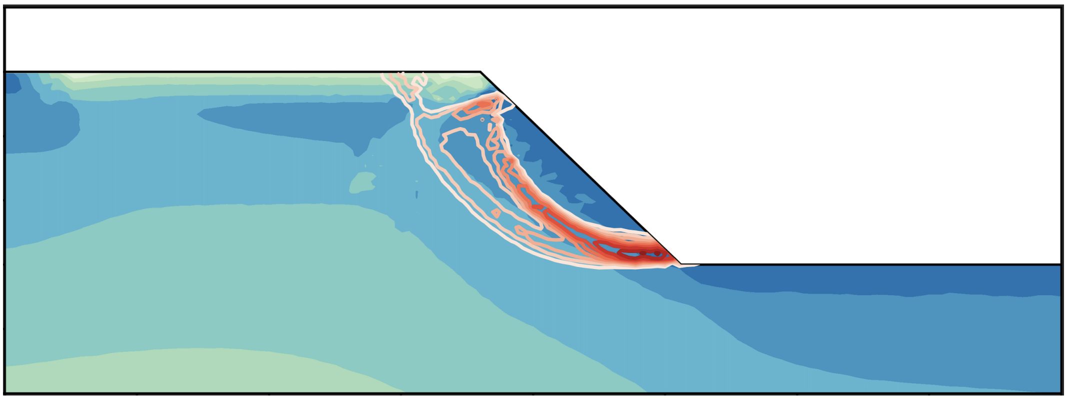

Hydraulic Impact of Vegetation on the Stability of Shallow Clay Slopes

Nature Based Solutions for Mitigation of Erosion in Göta Älv

Master's thesis in Infrastructure and Environmental Engineering

MARIA MARGENBERG
AXEL PERSSON

DEPARTMENT ARCHITECTURE AND CIVIL ENGINEERING
CHALMERS UNIVERSITY OF TECHNOLOGY

Gothenburg, Sweden 2022
www.chalmers.se

Master's thesis 2022

Hydraulic Impact of Vegetation on the Stability of Shallow Clay Slopes

Nature Based Solutions for Mitigation of Erosion in Göta Älv

MARIA MARGENBERG, AXEL PERSSON

CHALMERS
UNIVERSITY OF TECHNOLOGY

Department of Architecture and Civil Engineering
Division of Geology and Geotechnics
Chalmers University of Technology
Gothenburg, Sweden 2022

Hydraulic Impact of Vegetation on the Stability of Shallow Clay Slopes
Nature Based Solutions for Mitigation of Erosion in Göta Älv
Master's thesis in the Master's Programme Infrastructure and Environmental Engineering
MARIA MARGENBERG
AXEL PERSSON

© MARIA MARGENBERG, AXEL PERSSON 2022.

Supervisor: Jelke Dijkstra, Division of Geology and Geotechnics
Examiner: Jelke Dijkstra, Division of Geology and Geotechnics

Examensarbete ACEX30
Institutionen för arkitektur och samhällsbyggnadsteknik
Chalmers tekniska högskola, 2022 Master's Thesis 2022ACEX30
Department of Architecture and Civil Engineering
Division of Geology and Geotechnics
Chalmers University of Technology
SE-412 96 Gothenburg
Telephone +46 31 772 1000

Cover: Contour plot of a slope showing mean effective stress and incremental shear strain

Typeset in LaTeX
Printed by Chalmers Reproservice
Gothenburg, Sweden 2022

Hydraulic Impact of Vegetation on the Stability of Shallow Clay Slopes
Nature Based Solutions for Mitigation of Erosion in Göta Älv
Master's thesis in the Master's Programme Infrastructure and Environmental Engineering
MARIA MARGENBERG
AXEL PERSSON
Department of Architecture and Civil Engineering
Division of Geology & Geotechnics
Chalmers University of Technology

Abstract

Soil erosion is one of the drivers for landslides in natural slopes. In a climate where both high intensity rain and heavy wind is increasingly common, soil will erode more rapidly, especially in waterways. Traditional erosion barriers, such as rock revels or concrete walls, are not always suitable methods when considering downstream effects and ecological impact. This has led to an increased interest in combined or fully nature-based solutions (NBS). These methods incorporate vegetation to limit soil erosion. The body of the vegetation will reduce the speed of run-off, roots will reinforce the soil and evapotranspiration induces suction in the unsaturated zone, which increases stability. This project consists of a case study and a numerical analysis. The case study investigates four NBS constructed by the Swedish Geotechnical Institute (SGI) in Göta älv. Site visits, soil sampling and discussions regarding NBS for erosion mitigation were undertaken. These barriers attempt to reduce wave energy on riverbanks by different designs, which aims to allow vegetation to take hold. The study found lack of site data and limited time scope to be a hindrance in evaluating the NBS design. Leaning heavily on state of the art literature, suggestions are made to improve the design in future projects. The numerical analyses focused on the hydraulic effects of vegetation in an eroding slope by creating a Finite Element model of natural clay slopes with varying levels of suction and slope angles. This is to compare how failure mechanisms are affected by suction in the topsoil. An exponentially and a parabolic decaying root distribution is compared in a factor of safety analysis which is then related to the evolution of shear bands. The differences in factor of safety were found to be small between the two root distribution geometries, this may be explained by the high water table and small root depth. The analysis show a clear diffusion of slope failure mechanisms as shear bands that are clearly defined without suction are scattered into multiple potential slip surfaces when negative pore pressures are present in the topsoil. These shear bands merge into one band that is generally shorter and shallower than for the bare slope, which has a positive effect on the factor of safety. An increase in factor of safety between 25% and 45%, depending on the amount of suction induced, for a steep slope, is observed. The increase in stability attributable to suction is less prominent at gentle slope angles.

Keywords: soil suction, slope stability, nature based solutions, NBS, erosion, vegetation, shear bands, sediment transport, landslides

Hydraulisk Påverkan Från Växter på Stabiliteten för Grunda Slänter i Lera
Naturanpassade Erosionsskydd i Göta Älv
Examensarbete inom masterprogrammet infrastruktur och miljöteknik
MARIA MARGENBERG
AXEL PERSSON
Institutionen för arkitektur och samhällsbyggnadsteknik
Avdelningen för geologi & geoteknik
Chalmers tekniska högskola

Sammanfattning

Erosion är en av de stora drivkrafterna för jordskred, när skyfall och kraftiga vindar blir alltmer vanligt i framtiden kommer erosionen vid vattendrag öka. Traditionella erosionsskydd, som sprängsten och betongkonstruktioner, kan ha negativ ekologisk påverkan och negativa effekter nedströms. Detta har bidragit till ett större intresse för kombinerade eller helt naturbaserade lösningar. Dessa lösningar använder växtlighet för att minska jordrörelser. Växter ger en minskning av avrinningshastighet, rötter förstärker jorden samt evapotranspiration ger negativa portryck i den odränerade zonen vilket förbättrar stabiliteten. Projektet består av en fallstudie och en numerisk analys. Fallstudien undersöker fyra naturanpassade erosionsskydd uppförda av Statens geotekniska institut (SGI) längs med Göta älv. Platsbesök, upptag av störda jordprover och diskussion kring erosionsskyddens utformning har utförts. Tanken bakom skyddens utforming är att minska vågenergin som påverkar strandkanten, detta ska förhoppningsvis leda till ny växlighet på strandkanten. Målet med att utvärdera skydden begränsades av bristen på data och det korta tidsintervallet för det här projektet. Utifrån litteraturstudien föreslås förbättringar i designen för framtida liknande projekt. Den numeriska analysen fokuserar på hydrauliska effekter från växter i en eroderande slänt genom att sätta upp en finita element modell (FEM) för slänter med varierande släntlutning och storlek på negativa portryck. Detta för att jämföra hur drivkrafterna för skred påverkas av negativa portryck i de ytliga jordlagren. Säkerhetsfaktorn för ett exponentiellt avklingande och ett paraboliska rotsystem jämförs vilket kopplas till uppkomsten av skjuvband i slänten. Skillnaden i säkerhetsfaktor mellan de två typerna av rotsystem ses vara låg, detta kan möjligtvis förklaras av den höga grundvattennivån och det grunda rotdjupet i modellen. Analysen visar en tydlig skillnad mellan drivkrafterna som påverkar slänternas instabilitet när skjuvbanden är tydligt definierade utan negativa portryck och betydlig mer utspridda skjuvband som uppkommer när negativa portryck finns i de ytliga jordlagren. När skjuvbanden för slänter med negativa portryck sammangår till ett unisont band är de generellt kortare och grundare än för slänter utan växtlighet, vilket har en positiv effekt på säkerhetsfaktorn. En ökning av säkerhetsfaktorn mellan 25% till 45%, beroende på storleken av portrycket, kan ses för en brant slänt. Denna effekt är lägre för flacka slänter.

Nyckelord: negativa portryck, släntstabilitet, naturbaserade lösningar, erosion, växter, skjuvband, plaxis

Acknowledgements

This project was carried out during the spring of 2022 as the final semester of our Masters' programme at Chalmers. It is based on a topic suggested by SGI, Per Danielsson and Dominika Nordh at SGI contributed with the case study site and insightful discussions regarding the implementations of nature-based solutions, for which we are thankful.

We also would like to extent a warm thank you to Hanna Karlström at AFRY for her interest, support and discussions during the project. Additionally we express our deepest appreciation to our supervisor and examiner Jelke Dijkstra for the never-ending ideas, constant enthusiasm towards the subject matter and a helping talon in the geotechnical jungle.

Finally, we would like to acknowledge our friends and classmates that have made our time at Chalmers a most memorable one.

Gothenburg, June 2022
Maria Margenberg, Axel Persson

Notations

Abbreviations and acronyms

CRS	Constant rate of strain
FBM	Fiber Bundle Model
FOS	Factor of Safety
NBS	Nature-Based Solutions for erosion control
OCR	Overconsolidation ratio
POP	Pre-overburden pressure
PSD	Particle size distribution
RAR	Root Area Ratio
SGI	Swedish Geotechnical Institute
WWM	Waldron and Wu model for maximum root reinforcement

Parameters

α	Empirical van Genuchten parameter
c	Cohesion
c_r	Root reinforcement cohesion component
c'	Effective cohesion
F_s	Factor of safety
g	Gravity acceleration vector
$\overline{h}$	Head value
$\lambda*$	Modified compression index
$\kappa*$	Modified swelling index
I_p	Plasticity index
K_{0NC}	Jaky's coefficient of earth pressure at rest
k	Permeability

k'	Multiplication constant accounting for root orientation
k''	Specific multiplication constant accounting for non-simultaneous breaking of roots
m	Empirical van Genuchten parameter
M_c	Critical stress ratio at triax compression
M_0	Constant constrained modulus prior yield
M_L	Confined modulus post-yield
n	Empirical van Genuchten parameter
p_{active}	Active pore pressure
p_{steady}	Steady pore pressure
p_{water}	Pore water pressure
q	Specific discharge
R_a	Root area ration
S_{eff}	Effective saturation
$t_{r,u}$	Root tensile strength
ρ	Density of soil
ρ_w	Density of water
v	Poisson's ratio
v_{ur}	Unloading/reloading Poisson's ratio
w_L	Plastic limit
w_p	Liquid limit
γ	Saturated unit weight
γ_w	Unit weight of water
σ'_c	Pre-consolidation pressure
σ_v	Vertical stress
σ'_v	Vertical effective stress
σ'_{vc}	Vertical component of pre-consolidation pressure
ϕ'	Friction angle
ψ	Dilatancy angle
η	Factor of safety
θ	Water content
θ_r	Residual water content
θ_s	Saturated water content
$\underline{\nabla}$	Gradient of pore pressure

Contents

List of Figures

List of Tables

1

Introduction

In Sweden there are many cities located along waterways. The water provides an attractive environment for settlement for various reasons, but induces an increased vulnerability to natural hazards; flooding, loss of land through erosion and landslides to name a few. In western Sweden especially, numerous cities are built on soft clay deposits, and soft soil deposited in marine, river or lake environment which is common in the area, are often especially sensitive which amplify these risks. As climate change contributes to more extreme weather events, the risk of these hazards is likely to increase in the future. One of the two focal points of this study is erosion in Göta älv and how problems related to soil erosion can be mitigated by nature-based solutions. Nature-based solutions for erosion control (NBS) are measures that use ecological means to protect against beach erosion from wave action and river flow. NBS can also contribute to a local aquatic environment where vegetation and biological activity can thrive [17], in contrast to traditional methods. In addition, the NBS can provide improvements to slope stability [16].

The current Swedish guidelines for erosion mitigation measures, from 1987, cover the design of traditional bed and shore protection [72]. This method is often ecologically unfavourable, especially in smaller streams. Ideally mitigation measures should be environmentally non-intrusive and cost-effective, this brings the need to investigate new possible solutions for dealing with erosion. New solutions should be able to exist in harmony with the environment, limiting the negative impacts while improving the ecological environment [17]. There is a prominent lack of Swedish guidelines regarding NBS, this impedes the implementation of these solutions. An established framework and clear guidelines could contribute to a greater implementation in projects.

The second focus of this project is on hydraulic changes in soil as a result of vegetation, which is studied in a numerical analysis. Plant evapotranspiration decrease pore pressures in the unsaturated zone of soil, these negative pore pressures are called *suction*. While the mechanical effects of vegetation on soil stability are somewhat understood, the hydrological impact of evapotranspiration is less studied [85]. This leads to a difficulty quantifying the benefits of vegetation in slope stabilisation. This project tries to study the interaction between slope stability, erosion and vegetation by implementing the hydraulic boons of vegetation in the topsoil layer of a slope to explore any influence this has on slope stability and failure mechanisms. This is repeated for gradually steeper slopes and varying levels of suction.

1.1 Aim and objectives

The aim of this thesis is to quantify and model the hydrological effects of vegetation on slope stability in a setting of active erosion. Additionally, a literature review and case study will be undertaken to evaluate the design of NBS constructed by SGI in Göta älv. The goal by this is to identify potential improvements that can be made to the design of NBS constructed in the area in the future.

Research questions

The following research questions will be investigated:

- How is the global stability of a shallow clay slope affected by the hydraulic effects of vegetation located on the slope surface? Does the slope inclination affect the vegetation - slope interaction?
- Is there a change in failure mechanisms of a slope affected by negative pore pressures in the topsoil?
- Are the NBS constructed by SGI suitable for attenuation of the eroding forces present in the area? Are there considerations that should be made if more NBS are to be constructed in similar conditions?

Limitations

The main technical limitation in this project is lack of model input data at the two sites studied. This means that a literature review will be the basis for evaluating the four NBS built in Göta älv. The numerical analysis in the project will hence be of a general nature, and the focus will be to investigate the hydrological effects of NBS in an eroding slope. Input data will be gathered from several sources; local site investigation data from a nearby area will be used when possible. Otherwise, model parameters from previous studies in similar conditions will be used or empirical relationships.

Biodiversity and the ecological sustainability are motives for using NBS solution instead of traditional solutions, but to limit the scope of this project the biological aspects of the mitigation measures will not be investigated. Focus will be solely on geotechnical functionality.

Erosion will be studied and taken into consideration when discussing the functionality of NBS. In the numerical analysis erosion will be taken into consideration in a strongly simplified manner and no calculations of material erosion are made, instead erosion is modelled by an iterative increase in slope angle. The numerical model is created in 2D, thus simplifying both root and slope geometry. No 3D effects will be considered in the analysis.

Only matric suction is dealt with in this study, osmotic suction stemming from salt in the pore water is not considered.

1.2 Methodology

The first and second research question are addressed by a numerical analysis, modelling an eroding slope that is affected by suction in the topsoil. Factors of safety for different slope angles and varying levels and distribution of suction can be compared and discussed.

The third research question is dealt with through site visits, discussions with SGI and a literature review attempting to find state of the art design principles applicable to the setting at hand. A discussion and comparison between the sites and the literature will be the result of this part of the study.

2

Theory

This chapter describes information found in the literature review. Topics covered include hydromorphology, the formation of sediment, sediment transport, initiation of motion, slope stability, the effect of suction on soil, soil bio-engineering and erosion mitigation measures. The chapter aims to provide a solid background, covering aspects central to the study and technical details relating to both the modelling phase and the case study.

2.1 Hydromorphology

The formation of sediment

There exist three distinct categories of rock: igneous, sedimentary and metamorphic. Igneous rock is formed when magma or lava originating from the earth's subsurface cools, crystallizing the rock mass. Sedimentary rock is formed through the compaction and cementation of weathered rock or particles with organic origin, in a process called lithification. Metamorphic rock is formed when a rock is subjected to elevated temperatures and/or pressure, which breaks down the mineral components of a rock to form new distinct ones [34, 46]. The cycle of rock formation and break down is visualised in Figure 2.1.

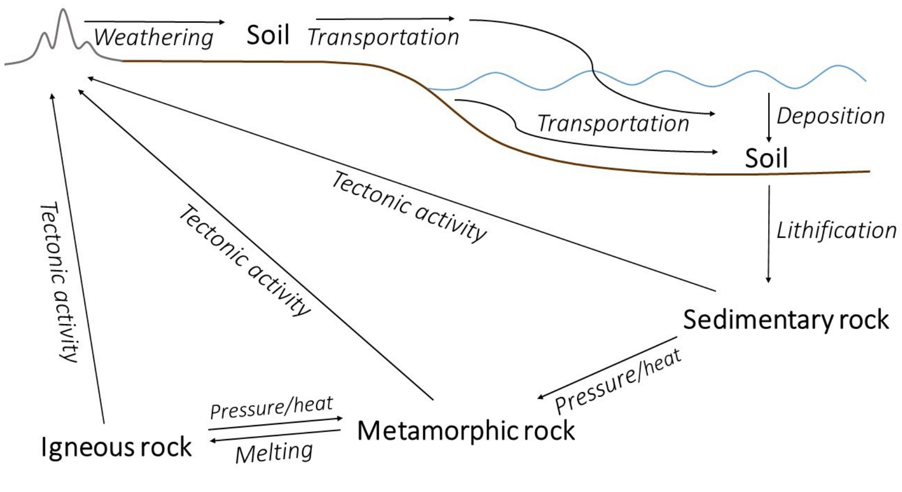

Figure 2.1: Illustration of the rock cycle recreated by A. Persson from [34]

.

Sediment particles are created by the weathering of rock, which can occur in several ways: by wind, water, tectonic activity, changes in temperature or by chemical processes. Once a rock mass has started to break down, rock fragments can be transported by water or when fractions reach small enough size, carried by the wind from their place of origin. The process of sediment transportation, in addition to moving soil, also creates a sorting mechanism. Since the force required to move a piece of rock will directly correlate to its size, density and porosity, a river will not transport all rock fragments equal distance and at equal speed [13, 34]. This leads to finer sediments being carried further while larger and heavier rock fragments may be left behind in a riverbed. After an extended period of time all of the finer sediments that once existed in the upper regime of a river system may have been flushed downstream.

It is generally true that the kinetic energy of the flowing water will reduce downstream as the topography levels out towards the river delta, though some authors [13] argue that this view is too simplistic, for example in places that are currently experiencing tectonic activity. Regardless, the kinetic energy, governed by the hydraulic and geometric conditions, will at some point be so low that even the finest sediment will stop moving and sink to the river or ocean bed, which is called deposition [17]. When many particles deposit at the same area a layer of soil will build up. If conditions change, for example during a period of heavy precipitation and river discharge, the soil can start to erode as particles are lifted from their deposited positions and transported by water or air [30]. This is highly idealized and in fact deposition, erosion and transportation will co-exist at any point in a river system.

The sediment exchange is the balance between deposition and erosion, areas with net deposition will experience build up material and areas with net erosion with lose material [13, 27]. Bed material loss or gain leads to changes in the bathymetric state, the boundary of the river. As such, no external influence is required for the conditions governing the sediment exchange balance to change - rivers will morph as a natural part of the rock cycle.

Sediment

Soil is classified into categories depending on sediment *particle size distribution* (PSD) as this property is a major indicator of the hydro-mechanical behaviour of a soil, albeit not the sole characteristic required to predict soil behaviour [5, 34]. Generally, soil whose properties are determined mainly by its content of clay and silt are considered *fine-grained*, while soils which properties are determined by its content of sand and gravel are considered *coarse-grained*. A more detailed description can be given based on the PSD. For this purpose, a range of systems exist, and naming is commonly based on percentage thresholds of particle content within classification boundaries [34], an example of which is presented in Table 2.1 according to the international European standard SS-EN ISO 14668 [39].

For clay the Atterberg limits gives a better indication of the classification than the particle size [59]. Fine-grained soils can behave plastically because of water existing under negative pressure in the very small pore space between particles [34].

Table 2.1: Soil particle classification, SS-EN ISO 14688-1 (2002). Upper fraction size limit in [mm] [39].

Clay	Silt	Sand	Gravel	Cobbles	Boulders
≤ 0.002	0.063	2.0	63	200	630

The strength that a fine-grained soil experiences as a result of this capillary pressure is referred to as cohesion and this behaviour is not observed in coarser grained soils which strength overwhelmingly stem from interparticle friction [34]. The plastic response of a fine-grained soil is dependent on liquid content, plastic limit (w_P) and liquid limit (w_L) of the soil, and a plasticity index (I_P) is defined in Equation 2.1:

$$I_P = w_L - w_P \tag{2.1}$$

This is the ratio of mass of water to mass of soil matter for which the soil exhibits plastic behaviour. A ratio lower than I_P would cause the soil to crumble and ratios above I_P would cause the soil to behave like a liquid [34]. Fine-grained soils are often classified further by determining the relationship between the plasticity index and the liquid limit. Santamarina [58] goes into detail describing soil as a granular matter, arguing that to understand soil behaviour one must understand particle behaviour.

Capillary forces were mentioned as playing a meaningful role in fine-grained soil behaviour, but there are several forces that interact with each other to create a distinct soil response, Santamarina [58] categorizes these forces three groups. *Particle level forces* are forces that a grain of soil can experience in the absence of other grains, these include gravitational and buoyancy forces. *Contact level forces* act between particles. Examples include capillary, electrical and cementation forces. *Boundary forces* are transferred through the soil skeleton in particle-to-particle chains from stresses on the boundary of the soil mass. The interaction between forces and ultimately the relevance of force groups on particle behaviour is what should decide particle classification argues Santamarina. As particle size increases weight and boundary forces will have increasing relevance with compared to contact level forces. Reversed, at small enough particle size contact forces prevail over particle forces. The transition point where dominating forces change from skeletal boundary to contact level is at $d \approx 10 \mu m$ [58] which is the particle size corresponding to medium silt [34, 58]. In other words, this is the point where a particle should go from being considered coarse-grained to fine-grained. The magnitude of boundary (skeletal), contact (capillary and van der Waals) and particle forces (weight) are compared for increasing particle diameter in Figure 2.2, assuming a spherical particle.

Pore fluid ionic concentration at small particle size will significantly alter electrical force conditions so that a soil formed in seawater will have different attributes than one formed in freshwater. Pore fluid replacement or leeching can change particle force balance after deposition, creating an unstable soil fabric [58]. The underlying mechanics and chemistry that control soil behaviour is demonstratively complex, and simply classifying all fine-grained soil as cohesive, as is industry custom, is misleading. Santamarina instead advocates for a nuanced understanding of particle states and interactions, rather characterizing soil as a mass in broad terms, as this should aid

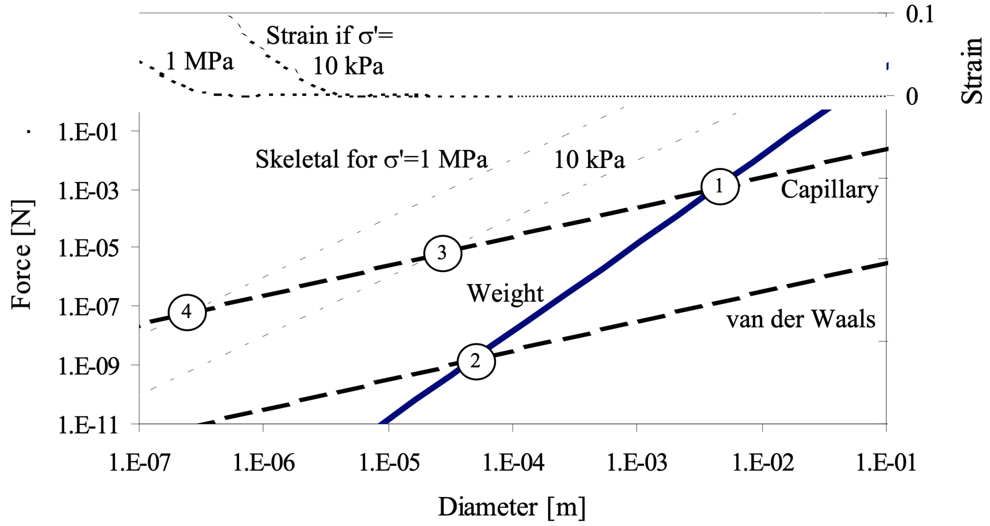

Figure 2.2: Skeletal vs contact forces [58]. The top part of the figure shows strain response from changing pore fluid from fresh-water to seawater.

in deciphering soil behaviour.

Sediment Transport

Generally, sediment transported in a river can be classified as either part of the *bed load* or the *suspended load*. The bed load is made up of larger particles that roll, slide or bounce off the riverbed, with frequent contact with the bed. The suspended load is made up of particles suspended in the water through turbulent movement with no meaningful contact with the riverbed [30]. There is no clear distinction in nature between these categories and a third category has been suggested [77] called the *saltation load* which attempts to capture particles that are in between these two distinctions, making longer jumps than bed load particles but that have less suspension time than the suspended load. Several different characterisation criteria have been suggested, for example based on maximum particle jump length and depending on which definition is used, saltation load may be part of the suspended load - an approach suggested by Einstein and Washington [22].

The separation of transport modes is important because there is no known relationship between the mechanisms controlling the two modes and as such, attempts to formulate equations that predict sediment transportation have done so by looking at each mode as its separate problem. A difficulty arise here though as no universally agreed definition of transport modes exists, meaning defining the scope of sediment transport prediction is a hurdle to get over in and of itself [75, 77].

Bagnold [5] suggests a differentiation based on whether the contact a particle has with the bed is limited by gravitational forces or by the effect of turbulent eddies in the fluid, in which the bed load categorisation is the former and the suspended load the latter. This approach was adopted by Van Rijn [77]. A particle will stay in suspension if the vertical velocity caused by random turbulence in the fluid is larger than the fall velocity of the particle [76], which for fine sediment (< 100

μm) can be described by Stokes law [30] in equation 2.2. This is also the basis for characterisation of fine material using sedimentation analysis to determine the particle size distribution.

$$w_s = \frac{gd^2}{18v}(S-1) \tag{2.2}$$

in which w_s = fall velocity, g = acceleration of gravity, S = specific density, v = kinematic viscosity coefficient, d = particle diameter. Corrections have to be made if the sediment concentration is high however, as the fall velocity will be lowered by interparticle interactions [30, 76].

Despite efforts, a theoretical relationship linking the total sediment load to flow velocity and sediment material properties has not been found. Thus, different empirical or semi-empirical equations have been developed to attempt to predict and model sediment transportation for the different modes of transportation [30, 68]. In 1984, Van Rijn developed two equations to calculate bed load and suspended load transport in m^2/s. These equations use various flow, fluid and particle parameters as input data and after calibration managed to predict sediment transport rates within a factor of 0.5 - 2.0 compared to measured values 77% of the time for bed load transport and 76% for suspended transport. The conclusion reached by Van Rijn [76] and other authors [13, 30, 43] is that accurate predictions of total sediment transportation cannot be made as the accuracy of controlling parameters is too low and the co-existence and interaction of both modes is not well understood.

Seepage is the movement of fluid through the pore space under a hydraulic gradient [34]. This flow induces a drag force on soil particles, which is counteracted by the weight of the particle and, for fine particles, van der Waals electrical forces of attraction. A loss of equilibrium will lead to a migration of particles. This form of erosion is called flushing and is only possible under relatively high water velocities that may occur in material with sufficient hydraulic conductivity, such as sand or coarse silt and under a high hydraulic gradient [58]. Furthermore, in order for the detached smaller particles in the soil to fit between pores formed by larger particles and be transported away, the soil must have a distribution that satisfy the particle diameter ratio $d_{large}/d_{small} > 15 - 30$, else clogging of the pores may occur instead leading to irregularities in pore water pressure [58].

When concerned with erosion of soil, initiation of motion is a key part of the transportation problem, as this describes the moment when a particle detaches from the bed or bank and moves downstream. This the part of the transportation problem is unfortunately one of the least studied and understood, in particular in regard to fine-grained sediment [30].

Initiation of motion

In the 1930s Shields [60] found an empirical relationship between particle Reynolds number and a parameter dependent on bed shear stress, sediment and fluid properties. This relationship meant one could predict the flow velocity at which detachment would occur based on sediment, fluid and flow properties. The problem is one of force equilibrium, where the water is subjecting the particle to some shear force and the grain has some resistance of movement that was said to be proportional to the weight of the grain. The relationship is plotted in figure 2.3 and is still the most used method of estimating the initiation of motion of sand particles [14]. However, the relationship is not valid for fine-grained sediment, as cohesive contact level forces are not considered [78]. A similar general relationship between material, fluid and flow properties and the detachment of a fine-grained particle has not been found and empiricism combined with extensive *in-situ* investigations are required to predict the critical shear stress at which a fine-grained particle detaches [5, 27, 30, 77].

There exists a long history of study in the subject of critical water velocities in relation to particle detachment, Brahms published equations relating to the topic in 1757 [12], but this natural process when concerning fine sediment has eluded accurate and general prediction still at the time of writing in 2022. A summary of the main difficulties encountered when attempting to create models of prediction for the threshold of motion for a fine-grained particle follows.

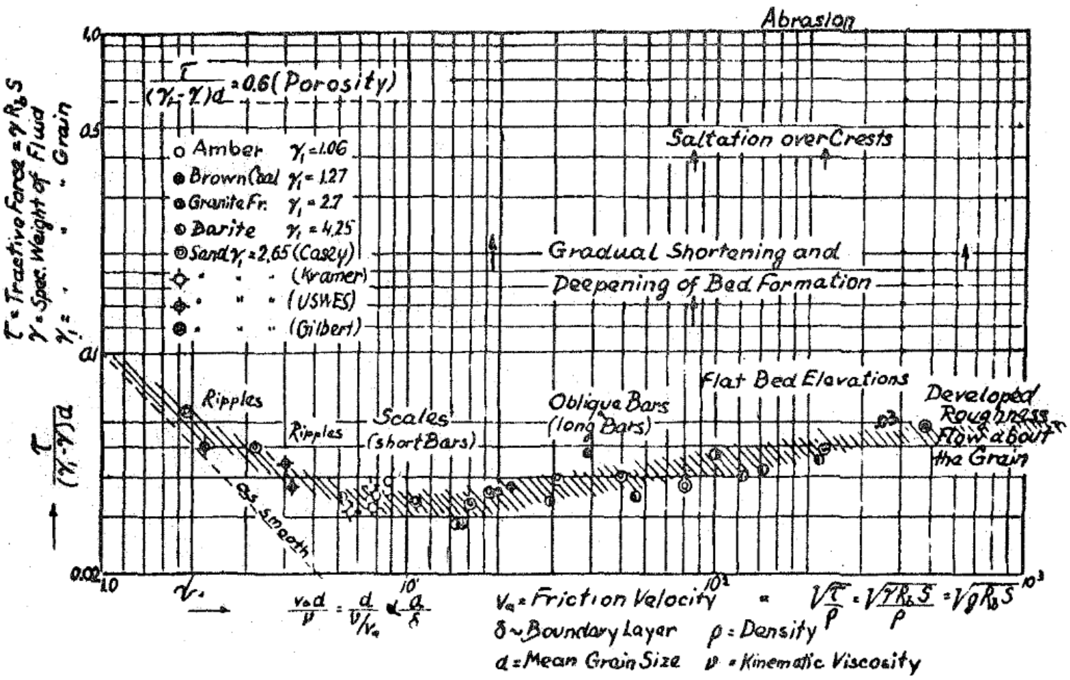

Figure 2.3: Shields [60] diagram published in 1936 comparing tractive force coefficient with particle Reynolds number.

The relevance of small turbulent eddies increases as particle size decreases [13, 62]. This increases the complexity of the problem as the stochastic nature of turbulent fluid motion makes calculations and accurate predictions difficult to make [19]. To address this a reference value is often used to determine the threshold of motion in fine-grained sediment, as a single grain could be moved at incredibly low flow velocities under the impact of turbulent fluid movement [43]. This reference erosion rate has traditionally been set to 10^{-6} m/s of average incremental erosion depth over time increment during which shear stress has been applied.

The relevance of inter-particle contact forces on a particle's resistance to movement will become dominant over gravitational forces at particle sizes smaller than silt, as seen in Figure 2.2. In a study attempting to adapt the Shields curve (Figure 2.3) for sand with silt content it was found that the specific PSD of the mixed material has a huge impact on critical shear stress [42]. It was also concluded that the relationship found for silty sand is not valid for clayey sand, likely as the attraction and repulsion forces in the soil will have different mechanisms for these fractions [42]. The lack of understanding and generality in models regarding these contact level forces makes the problem yet more complex and often cohesive and adhesive forces need to be measured in-situ and cannot be derived from material relationships directly [13, 30]. The equipment required to measure such properties is not commonly available [27], further complicating the prediction process.

True for initiation of movement of both coarse-grained and fine-grained soil is that most existing models and indeed the ones described so far have been created to predict particle movement in a bed of a river as a result of shear stress imposed on a particle from a flowing fluid. In the present study however, a riverbank is concerned and as such additional stresses will affect particles on the slope, perhaps from ship waves in particular, but also run-off, rain impact and wind. It is evident that the present study cannot attempt to predict the pattern of erosion at the site in question, but this summary of the erosion prediction research and its cruxes will be helpful when evaluating measures to hinder the movement of soil.

2.2 Slope Stability

The stability of a slope is determined by the equilibrium of the driving forces and resisting forces, failure occurs when the shear stress in the soil exceeds the available shear strength [34]. The relationship can be characterised by a factor of safety that indicates if there is a risk of failure, this can be expressed as the force equilibrium in Equation 2.3:

$$F_s = \frac{\sum stabilizing forces}{\sum overturning forces} \tag{2.3}$$

If the safety factor is larger than one, the slope can generally be considered stable [34]. This relation is not only influenced by the soil properties but the water table, gravity, seepage forces and any seismic activity as well. Potentially unstable soil masses could be created by either natural processes such as erosion and deposition of materials, or human activity as excavation and construction [44]. Stability analyses can be done through various methods such as the limit equilibrium method (LEM), discontinuity layout optimisation (DLO) or the more advanced finite element modeling (FEM) [34].

The finite element method is a numerical method that can simulate the non-linear hydro-mechanical behaviour of soils, compared to the limit equilibrium method this allows for more advanced models that capture the deformations and evolving state, such as (effective) stress and pre-consolidation pressure [25]. The development of more powerful computational tools has allowed the methods used for slope stability calculation to be more advanced than previously possible.

When considering clay, the shear strength is dependent on the drainage conditions. In undrained condition, excess pore pressures are not allowed to dissipate, characteristic short term behaviour [34]. For a characteristic long-term behaviour, where excess pore pressure has been allowed to dissipate, a drained response is induced where the cohesion and friction angle is expressed as effective parameters c' and ϕ'.

An induction of negative pore pressures, *suction*, will influence the behaviour of the soil. A high water content, and a low suction, generates lower apparent soil cohesion [24]. Low water content, and high suction, gives a stronger apparent cohesion and a lower landslide risk. For natural slopes the soil moisture and saturation will vary with the topography [53].

Leroueil [41] divide the failure of a slope into four stages:

- Pre-failure: deformations proceeding the failure due to change in stresses, creep, strains and displacements linked to progressive failure.
- Onset of failure: formation of a shear surface through the soil mass.
- Post failure: the movement of soil mass from the landslide until it completely stops.
- Reactivation: the sliding of soil mass along a existing shear surface.

The pre-failure behaviour within the soil first described by Terzaghi [69], results in a reduction in shear strength along the shear surface. The deforming material then undergo pre-failure creep in three phases of strain development [38]. The strain rate have been found to increase when approaching failure [41].

Slope failures can be divided in the following types of behaviour: *rotational*, *translational* and *compound slips*. The rotational slips appear as a circular or non-circular curve. Circular slips are often associated with homogeneous anisotropic conditions while non-circular slips is linked to non-homogeneity in the soil. Translational or compound slips appear when the failure surface is influenced by adjacent layers with a significant difference in strength [34]. Therefore, the anisotropy of the soil is of high interest when investigating the slope stability.

The formation of *shear bands* is the localisation of deformations in a band preceding the shear failure of soil [45]. The spontaneous formation of shear bands in sand has been studied in the early work by Vardoulakis [79], shows that the localisation in biaxial test, plain strain, is only possible before the plastic limiting state and that the approximated inclination is given by the formula proposed by Arthur et al. [3]. The location of the shear band can through the formula be estimated from the the peak friction angle and dilantancy angle [3].

Desrues et al. [20] have performed more recent studies on the deformation band using a newly-developed triaxial cell and a specifically designed x-ray scanner. This allows for smalls steps of strain to be applied between scans, making it possible to follow the progressive failure mechanisms more thoroughly than before. The study shows that the strain localisation appear early in the tests. The observed shear bands appear gradually - no defined moment can be found where the strain localisation starts [20]. From this, they leave the question open regarding how early the strain localises and suggest the development of more refined measurement tools that can register strain otherwise overshadowed by the numerical noise to be able to more clearly study these effects.

The recent advances made in the x-ray imaging technique, has further improved the possibility to observe deformation and fabric evolution in geomaterials [10]. A very recent study by Birmpilis et al. aims to investigate the deformation response during a drained triaxial test on specimens of natural sensitive clay. This show that the stress ratio applied at the boundary will to a large extent govern the total volumetric strain and total deviatoric strain. The phenomenon can also be studied numerically through FEM analysis [38]. Although new advances, the development of shear bands in naturally structured clay with high sensitivity lacks of comprehensive understanding [45].

Erosion and Slope Stability

The main control of slope instability is through the critical slope angle. This critical angle varies greatly due to the shear strength, type of material and characteristics of the slope [73]. Modification of the slope profile through erosion and loss of support may cause a higher susceptibility for instability. There are several processes involved in the shaping of natural hillslopes with the main ones being: gravity, wind and running water. The slope process where gravity is the dominant driving force for transport are called mass movements. When other forces are dominant e.g., wind or water, the process is called erosion [73].

Due to the lack of an established relationship between erosion and bank stability this is usually simplified to be able to be expressed in a geotechnical model. This often result a simple geometry with homogeneous conditions and very simplified geomorphological conditions [35]. Lai et al. states that a model that combines vertical and lateral fluvial processes for geofluvial modelling is needed for accurate predictions but in 2014, at the time of their study, this was still at a research stage [35]. They also highlight the lack of appropriated models that can simulate bank retreat in a satisfactory way. In the study they try to predict bank retreat by developing a coupled model that include both a process-based bank stability model and a two-dimensional mobile bed load model. The model is finally verified against real measurements at Goodwill creek, Mississippi. There it can be seen that the two-dimensional model shows significant improvements when compared to the previously used one-dimensional models but they identify the need for additional improvements of the numerical models for complex streams. They also highlight that the simplifications made regarding constant elevation and horizontal groundwater table will lead to incorrect predictions of the timing of bank failure and further research is needed in this field.

In the models available today, the spatial connections between the floodplain components and how riparian plants alter the characteristics is neglected [55]. Further research in this field is needed to be able to develop robust models.

The Influence of Vegetation on Slope Stability

To be able to apply vegetation for slope stability in an engineering perspective there are concerns that needs to be highlighted. As described in Figure 2.4 there are three aspects that can be applied for restoration of slope stability [66]. The technical and socioeconomic principles are well described but ecological and ecophysiological aspect lack of established knowledge in an engineering perspective. Furthermore, the relationship between all corners of the pyramid needs better linkage. The longer the time scale of the project, the more essential will the ecological approaches become.

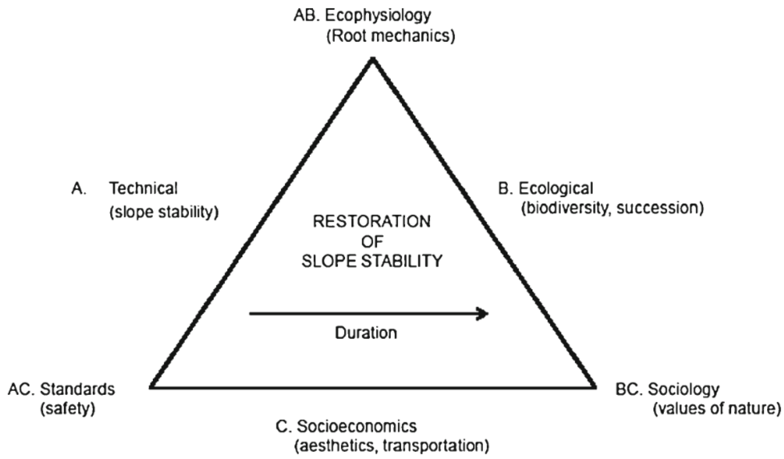

Figure 2.4: Aspects for slope stability restoration by [66].

Vegetation will impact the stability in several ways, altering both the hydraulic and mechanical behaviour of the soil mass. Depending on the species vegetation can have a variety of traits, with both positive and negative effects on slope stability. A summary of the engineering role of vegetation can be seen in Figure 2.5 [16].

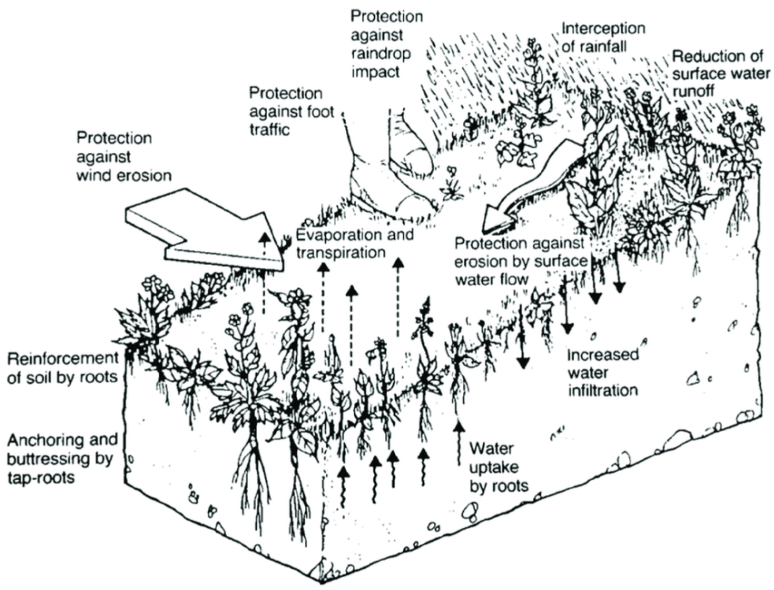

Figure 2.5: Influence of vegetation on the soil from [16].

Vegetation may provide a barrier between the soil and the forces that impact erosion or mass movement [63]. Thicker roots can act as nail spikes in the slope and thinner roots will, when located in the shear zone, reinforce the soil. This can increase the protection against shallow landslides [65]. For landslides with a deeper seated failure mechanism the effect of vegetation is limited. In addition to this the stem of the vegetation can provide support above ground, capture some of the eroding soil and intercept rainfall [63]. The uptake of water through transpiration will desiccate the soil and induce *suction*, a state of negative pore pressures in the soil. This hydrological effect will increase the shear strength of the soil and consequently the slope stability [26]. Vegetation can be used to increase the hydraulic roughness of a channel which reduces flow velocity. The hydraulic roughness of a vegetated channel feature is however drastically reduced when plants are submerged [44], meaning means less resistance to flow velocity and higher rates of erosion. Additionally species selection is important as some plants have been found to increase the turbulence in the flow [44] which may lead to increased erosion. Negative effects may also occur from vegetation, it can bring an additional load on the slope and roots can increase the infiltration and permeability of the soil. Table 2.2 shows a summary of the effects on slope stability by vegetation according to Morgan and Rickson [44].

Table 2.2: Effects of vegetation on slope stability, recreated from [44].

	Process	Type	Effect on stability
Roots	Increase permeability and infiltration and therefore the pore pressure	Hydrological	Negative
Roots	Transpiration gives rise to negative pore pressures - suction	Hydrological	Positive
Vegetation	Increase interception and evaporation, this reduces the pore pressure	Hydrological	Positive
Vegetation	Increase weight or surcharge, gives increased load on slope	Mechanical	Negative
Vegetation	Increases wind resistance, gives an increased load on the slope	Mechanical	Negative
Roots	Reinforce the soil, increase the strength	Mechanical	Positive

The mechanical and hydrological impact of vegetation on soil have mainly been studied separately, but there is an interaction between these processes and their impact can even offset one another [28]. Stokes et al. suggest using a multidisciplinary approach when investigating vegetated slopes, considering both physical and biological parameters [65]. But they also highlight the lack of models that are able to implement all these aspects and especially the difficulty in establishing the relationship and evolution of theses interactions over time. The influence of vegetation type on the stability of a planted slope, in regard to spatial-temporal effects on mechanical and hydrological properties are still insufficiently understood [66].

The mechanical effects of vegetation have been studied and can be somewhat represented in a simplified way in geotechnical modelling, although how well this represent the reality can as always be discussed as there are many site-specific conditions to consider [83]. Furthermore, the hydraulic benefit of transpiration on slope stability is one of the least studied effects that plants have on soil, and this will be the focus of the present study. At sites where the soil contains roots, the shear failure of the slope would also include the failure of the root-soil system.

Stokes et al. [65] reviews different approaches in modelling the mechanical reinforcement of the soil. The roots mechanical contribution can be modelled as additive soil cohesion in the Coulomb failure criterion. When considering an ultimate limit state, the peak mechanical reinforcement from roots can be expressed as an additional cohesion component c_r. The pioneering modelling work, suggested by Waldron [81] and Wu et al. [84] (WW model), describes the maximum root reinforcement by Equation 2.4:

$$c_r = k' \sum_i t_{r,u,i} R_{ra,i} \tag{2.4}$$

in which the maximum reinforcement is linked to root tensile strength ($t_{r,u}$), root area ratio (R_a) and the multiplication constant (k') accounting for root orientation [83]. As all roots are assumed to break at the same time, these early models have been shown to overestimate the additional cohesion due to tension. To account for the difference between this model and field measurement a site specific multiplicator factor (k''), ranging from $k'' = 0.3 - 1.0$, accounting for non-simultaneous breaking of roots has been implemented [6].

An alternative to the WW model is the improved model by [53] who applies a Fibre Bundle Model (FBM) on riparian vegetation. The FBM provide a more accurate estimation of root reinforcement as it considers the progressive root breaking during failure. Although FBM holds a better accuracy for modelling root reinforcement than WWM, several limitations still exist in the accuracy of the model. Some studies suggest using a root architecture model as an improvement for slope stability analyses including root systems [18, 54].

Vegetational Effects on Soil Suction

Evaporation and transpiration are the two vegetational processes that remove water from the soil, lowering pore water pressure [66]. Mechanisms that result in a lowering of the pore-pressure are favourable for the slope stability, especially for shallow landslides, and a higher pore pressure is generally unfavourable. As previously stated, the hydrological and hydraulic effects from vegetation are less studied than the mechanical effects acquired from root systems. The limited understanding of soil desiccation, root-water uptake and the effects from mixed species of vegetation limits the established practices in this area [49, 86].

The root morphology and soil compaction will affect the possible water uptake from vegetation. To complicate the generalisation of transpiration for different types of vegetation, root morphology is dependent on abiotic factors as well as the genetics of the species [86]. To clarify the architecture of different root systems four different root architecture patterns have been idealized, see Figure 2.6 [86]. The idealization can be seen over the horizontal extent x and to the root depth z_r.

The soil suction also affects the transpiration rates, greater soil suction leads to more difficulty for the roots to draw water from the soil. Soil suction can then be considered as a reduction factor of the maximum root water uptake [31]. The potential transpiration rate is hard to verify in measurements. Therefore, indirect estimates are conducted. Studies have been conducted to find how the magnitude of plant induced suction varies with a number of variables, and the amount of suction measured or analytically calculated varies greatly between studies.

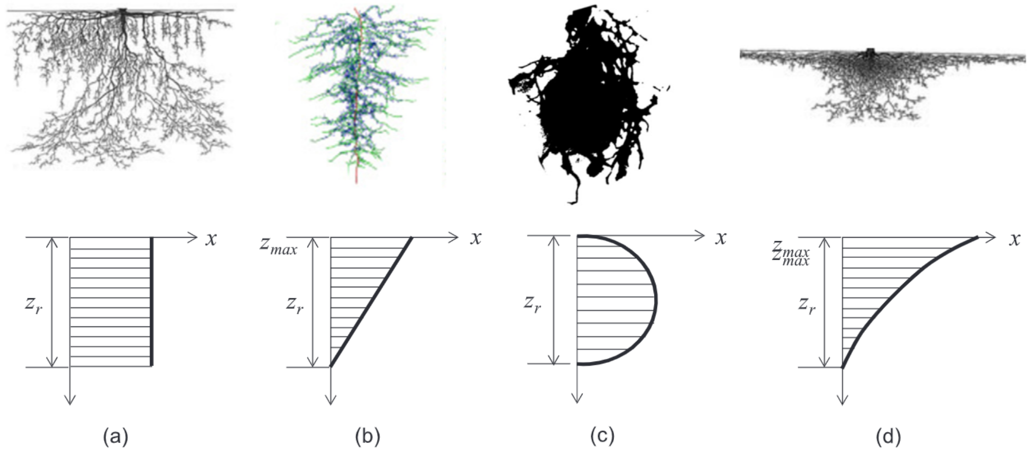

Figure 2.6: Root architecture and the idealized representation from [86]: a) Uniform distribution; large taproot and large horizontal lateral roots, b) Linearly decreasing distribution; taproot with small lateral roots, c) Parabolic distribution; concentrated roots system, d) Exponential decaying distribution; plane shaped root system.

The degree of saturation in the soil is the key predictor for soil suction as well as plant transpiration. In a flooded soil, anaerobic conditions will cause the plant respiratory process to slow down or stop, while at very low degrees of saturation a lack of available soil water will hinder transpiration and thus lower suction [86]. The highest amount of suction is found in a drying soil and as such soil suction in both a bare and a planted slope is highly cyclic. Several studies have been conducted to quantify the suction induced by soil and find relationships between species of plant and different environmental conditions. Zhu et al. [86] found that the maximum suction is reached at the surface for exponential root systems, but for parabolic root systems the maximum suction is reached at half the root depth. This is consistent with the results of Ni et al. which compares the suction in a mixed grass and tree planted slope to single species and a bare slope, where the parabolic root system of the trees studied reach peak suction at half the root depth [49].

Ni et al. also concluded that the tree-grass competition for water present in a mixed slope led to a higher peak suction than for the mono-species slope [49]. Trees will however shade grass and inhibit growth of biomass, meaning that ideally grass should be established before trees are planted. The peak suction varies between studies but generally lies between 20 and 200 kPa for a planted slope and 0 and 20 kPa for a bare slope as a result of capillary forces. [48] measured a peak suction of 50 kPa in a grass slope and 67 kPa in a tree slope compared to 6 kPa in a bare reference slope, for tests in a silty sand slope. From these results one can conclude that a combined tree/grass slope should reach suction levels above 67 kPa if all other variables are unchanged [48, 49]. From Zhu et al. [86] one can conclude that shallower root depth correlates with higher maximum suction, but the peak is reached at shallower depth. Both these studies investigate slopes in completely decomposed granite, a soil common in the Hong Kong area, and the particle size is mostly sand [49, 86]. The same tree is also studied, *Schefflera heptaphylla*, a woody plant species with quite shallow roots that is common in Asia.

Since soil types, available vegetation, climate and topography vary greatly across regions there is a need for research in hydraulic effects from NBS targeting Swedish conditions with the goal of creating clear design principles for engineers and groundwork contractors to employ. The lack thereof is a major hindrance in choosing NBS over traditional solutions for which clear design guidelines exist.

Types of Vegetation

This section describes the characteristics for different types of vegetation and how they can be used to mitigate erosion and improve slope stability. Species selection is very important as there are large differences in root system architecture, root tensile strength, biomass, growth time, transpiration levels, hardiness all of which will impact the effectiveness of a NBS. When possible, it is preferable to use native plants to avoid introducing invasive species [65]. Any long-term effects also need to be considered for the implementation to be viable and successful.

Grasses are quick growing and can provide a solid protection of the ground. As many species of grass have dense shallow roots these are useful in protecting sites from superficial erosion [64]. Even moderate damage to the plant will not result in lasting damage as fast regrowth will occur. Although most have shallow roots, some species are known for deeper root systems which also can be suitable in use for erosion control, one example of which is vetiver grass (*Chrysopogon zizanioides*) [65], commonly used for this purpose in tropical regions, shown in Figure 2.7.

Herbs can be both annuals and perennials. They usually grow close to the ground with shallow root systems providing a dense covering of the ground [64]. Some species have significantly deeper root systems giving a deeper stabilizing effect. Fast growing herbs can be useful when shallow reinforcement of soil is needed, in contrast to woody plants and shrubs that grow at a slower pace [65].

Woody plants have a perennial woody stem that support vegetative growth. Shrubs are low-growing woody plants with several stems. The height of shrubs can vary from 0.2 m to up to 6.0 m depending on species. Shrubs generally grow lower than trees and can be easier to maintain, but the root system will not reach as deep and far. Although, the tensile strength of the root system of shrubs is for some species comparable to trees [66]. Trees are perennial plants with a woody stem that support vegetation. Sizes can vary from smaller species up to several meters wide and high, with a great root depth. Trees can be suitable for use in slope reinforcement, but their use can also lead to the negative effects described in Table 2.2 [64]. It has been suggested that woody roots significantly reduce the landslide potential on shallow depth (<1 - 2m) on steep slopes. The woody roots are not considered to have any significant impact on deeper landslides (>5 m) as root density is quickly decaying and few roots are able to anchor across a deep failure plane [65]. Popular species of trees/shrubs are aspen (*Populus tremula*) and willow (*Salix alba*) as they easily propagate from cuttings or live poles. Example of a willow tree can be seen in Figure 2.8.

Figure 2.7: Vetiver grass [70].

Figure 2.8: Willow, *salix alba* [82].

2.3 Erosion Control

As stated by Danielsson et al. [17], the best approach is to avoid implementing measures for erosion control altogether as these impact the river morphology and local ecosystem. When measures are necessary to protect infrastructure or prevent the loss of land in otherwise vital areas, these should intrude minimally on the environment. Generally, measure for erosion control can be divided into three groups:

- Soft structures, e.g. live cuttings, wood.
- Hard structure, e.g. gabions, retention walls, anchors.
- Combined structures, a combination of the two above.

Traditional solutions are often considered to be hard measure while the nature-based solutions is considered soft or combined measures. Soft structures might take longer time to reach full stabilizing effect, because of slow vegetation growth, and are more suitable where slope instability is anticipated and not yet at a critical stage [66]. The longevity of soft structures is not studied to a satisfactory degree, more documentation is needed to be able to compare NBS to hard structures that have a documented lifespan of 50-100 years.

Traditional Solutions

The measures traditionally used in Sweden for protection of slopes are hard barriers such as stone cover, concrete mats or stone gabion walls. The current guidelines from 1987 only include the traditional hard types of protection in waterways [72].

These solutions provide a solid resistant protection against local erosion, but the implementation will have a significant impact on aquatic life [44, 50] and can cause elevated problems downstream. The application of hard barriers in sensitive areas might compromise natural values, and the environmental aspect is important to include early in a planning process [50].

Nature-Based Solutions

The use of vegetation for engineering purposes can be referred to as *bio-engineering*, a concepts that include traditional civil engineering knowledge as well as a more biological multidisciplinary approach. The aim of NBS, as with traditional erosion barriers, is to prevent erosion. The additional objective of NBS that is a shortcoming of traditional methods is to limit negative ecological and biological impacts and to create potential habitats [17]. The definition of NBS varies, but NBS are in this project considered to be measures to protect against erosion that incorporate vegetation in a structural way and through this aim to satisfy the objectives described.

There can be a difficulty in installing vegetation in critically degraded slopes due to poor soil conditions [66]. This can be improved by the installation of other engineering structures. The amount of knowledge in this field is limited for Swedish conditions but recently performed field experiments in the Swedish archipelago have successfully shown that a combination of a stabilizing structure and vegetation will mitigate erosion and further promote vegetation growth [2]. When choosing NBS method, site conditions needs to be thoroughly investigated for the barrier to be effective [32]. To follow is a review of common NBS and how they can be implemented:

Turfing consists of applying grass with developed roots onto the slope surface [44]. To be successful this requires that the slope is not to steep, at maximum an angle of 1:3. The method is not suitable for all soil conditions however, and turfing also requires maintenance in the early stages to make sure establishment of vegetation is successful, followed by continual minor maintenance. An example can be seen in Figure 2.9.

Figure 2.9: Example of turfing in a small stream [40].

Live or inert fascines and straw wattles is a method in which bundles of live cutting are placed in trenches across the slope, these are then fastened to wooden stakes [44]. Live fascines are meant to take root, providing additional stabilization, while inert facines are not. Fascines provide slope stabilization, additional drainage as well as erosion protection for low flow velocities [32]. This will slow over-bank erosion and provide some structural slope stability.

Live stakes are fresh cuttings from woody species that are installed along a slope. This method can also be combined with other techniques as it will take some time for the stakes to take root and become effective in stabilizing the slope. For some species of plants the reinforcement depth can be significant [32]. An example of live stakes can be seen in Figure 2.10.

Figure 2.10: Live stakes [47].

Branchpacking consists of alternating layers with live branches and compacted backfill which can repair local slumps or holes. This provides local mitigation and reinforcement but is not applicable in larger areas. The depth needed should be long enough to reach the undisturbed soil. This method could be combined with other methods as well [32], see Figure 2.13.

Live cribwall is an option when strong currents are present and other options might not be suitable. A cribwall is constructed of interlocking logs, timber, soil rocks, and live branches that forms a box to fill a bank. This is filled with soil material and cuttings are planted to act as support of the bank [32, 44]. A schematic picture can be seen in 2.11.

Brush mattress consists of living branches placed on the slope surface in a criss-cross pattern to form an immediate protection of the slope. Thereof is this a suitable method for fast flowing streams [44].

Coir rolls are cylindrical rolls of coconut husk fibre bound with coconut husk twine [32]. This can be made with or without pre-installed plants to help the vegetation establish faster, Figure 2.12. These can for example be anchored to slopes to mitigate erosion.

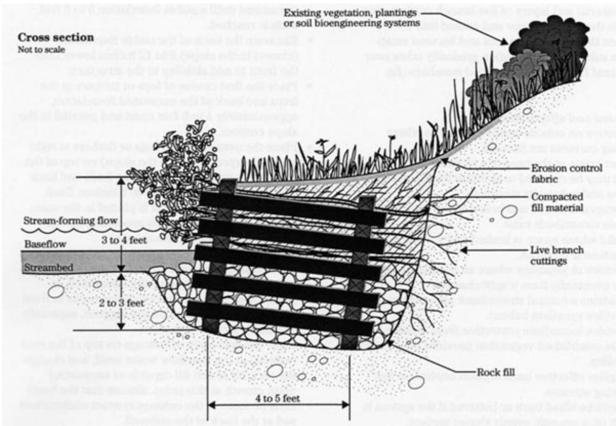

Figure 2.11: Live cribwall [71].

Figure 2.12: Pre-planted coir rolls [1].

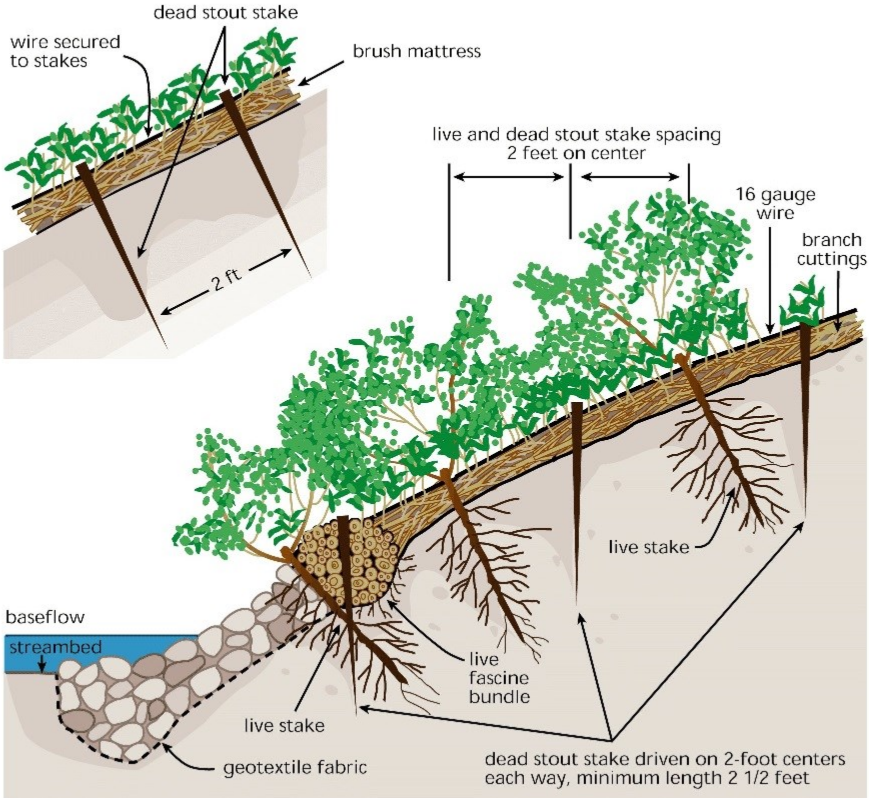

Figure 2.13: Example of brush mattress combined with other NBS [23].

2.4 Plaxis Implementation

This project uses the Finite Element software Plaxis to investigate the hydraulic effects of vegetation on slope stability. A *fully coupled flow analysis* and a *safety analysis* is performed to simulate suction effects and how this influences e.g. the safety factor.

Traditionally geotechnical problems have been solved using simplified analytical methods or empirical approximation, when geotechnical problems contain non-linear behaviour or other complex constrains numerical approximations are often necessary [33]. Plaxis is a FEM program developed for the solution of a variety of geotechnical problems and can provide solution for 2D problems as well as 3D [7]. This allows for the study of deformations, groundwater flow, dynamics and stability in a geotechnical engineering context. FEM allows for a continuum to be discretized into a number of elements and nodes [8], this allows for an approximate solution to be obtained for a boundary value problem.

In Plaxis the user can choose between 15-node or 6-node triangular elements [7]. The solution will be influenced by the number of elements used, a higher number of elements will give a solution with higher accuracy but this will prolong the calculation time. Several constitutive soil models can be utilized in Plaxis, each suitable in different conditions - depending on the soil behaviour that needs to be captured. A constitutive soil model is a generalised description of the stress-strain relationship, defining the incremental strain caused by the stress [33]. The result of a numerical analysis is highly dependent on the soil model as well as the quality of the soil sampling and testing.

For the present study, the Soft Soil model will be utilized for the clay material because of the light over-consolidation of the material and the short-term focus of the analysis. The Soft Soil model also has input parameters that are more easily derived when compared to similar alternatives, such as the Hardening Soil model [33].

Groundwater Flow

When considering a fully coupled flow analysis in Plaxis, the partially saturated soil becomes of higher importance and needs further attention than in an analysis only considering the steady state groundwater [7]. For this characterisation a *soil-water retention curve* (SWRC) is used, it describes the relation of suction and degree of saturation in the unsaturated zone [4]. There are several functions included in Plaxis for describing the flow behaviour in the unsaturated zone and the determination of the SWRC, of which the well known and established *van Genuchten* model is used in this project. The van Genuchten model determines a closed form equation for predicting the hydraulic conductivity in unsaturated soils, Equation 2.5 and 2.6 [74].

$$S_{eff} = \frac{1}{[1 + (\alpha h)^n]^m} \tag{2.5}$$

$$S_{eff} = \frac{(\theta - \theta_r)}{(\theta_s - \theta_r)} \tag{2.6}$$

in which S_{eff} is the effective saturation, θ is the water content, θ_r is the residual water content, and θ_s is the saturated water content, and h is the matric potential [kPa], lastly α, n and m ($m = 1 - 1/n$) are the empirical van Genuchten parameters.

For low to moderate suction levels the van Genuchten model provides fair solutions, but for high suction levels the suction remains at the residual saturation [9]. The functions can be defined by the user of by the predefined data sets available in the program, based on the soil PSD [7]. The pre-defined data sets allows for easier implementations for the user, requiring less input data, but it should be noted that these pre-defined data sets is only an estimate with limited accuracy.

The lack of data in this project have led to the use of these predefined data set, so the result might be influence by that. The USDA data set is based on the international soil classification system and allows for the implementation of the *Van Genuchten* or *Approximative Van Genuchten* model. The USDA data set with van Genuchten parameter's, implemented in this project, are based on the works by [15], estimating the variability for the uncertainty linked to water flow or solute transport in unsaturated soil. The saturated permeability k_x and k_y may be obtained through either the data set or the grain size distribution [7].

The flow in a porous medium can be described by Darcy's law, Equation 2.7, expressed in three dimensions [7]:

$$q = \frac{\mathbf{k}}{\rho_w^g}(\underline{\nabla} p_w + \rho_w g) \tag{2.7}$$

$$\underline{\nabla} = \begin{bmatrix} \frac{\partial}{\partial x} \\ \\ \frac{\partial}{\partial y} \\ \\ \frac{\partial}{\partial z} \end{bmatrix} \tag{2.8}$$

Where q is the specific discharge, $\mathbf{k}$ the coefficient of permeability, g the acceleration vector due to gravity and finally the density of water ρ_w. $\underline{\nabla} p_w$ in Equation 2.8 describes the gradient of the pore pressure that causes groundwater flow [7]. For unsaturated soils the coefficient of permeability can be related to soil saturation through the following Equation 2.9:

$$\mathbf{k} = k_{rel}\mathbf{k}^{sat} \tag{2.9}$$

for which k_{rel} is the ratio of the permeability at a given saturation to k^{sat} the permeability in saturated state.

There are several types of ground water boundary conditions that can be applied in Plaxis to simulate the geotechnical problem. A *closed head boundary* will be specified as a zero Darcy flux over the boundary as Equation 2.10 [8]. A closed head boundary is only applicable to the external boundaries of the model [7].

$$q_x n_x + q_y n_y = 0 \tag{2.10}$$

A *head boundary* can be prescribed as Equation 2.11, with a prescribed input head value $\overline{h}$:

$$h = \overline{h} \tag{2.11}$$

Any hydraulic conditions defined using the *flow boundary conditions* settings in Plaxis will prevail over the *model conditions* [7].

Definition of Stresses

The total stress consists of the effective stress and pore pressure. The pore pressure include the steady state pore pressure and the excess pore pressure, Plaxis denotes pore pressure contribution of the total stress by p_{active}, the *active pore pressure*, Equation 2.12 [7]:

$$p_{active} = S_{eff}(p_{steady} + p_{excess}) = S_{eff} p_{water} \tag{2.12}$$

Where p_{excess} is the excess pore pressure, p_{steady} the steady-state pore pressure and S_{eff} is the effective degree of saturation and p_{water} the pore water pressure. When the soil is fully saturated, $p_{active} = p_{water}$, but the clear distinction between the two is in the unsaturated zone [7]. For a *fully coupled flow analysis*, the assigned water conditions are taken into consideration at calculation step 0, calculating the output p_{excess} from the preliminary steady-state . In the following steps Plaxis performs the flow calculation based on the outcome of the previous step [7].

In Plaxis the soil material is regarded as a two-phase material, this can be done through the classical approach considering the Terzaghi's definition of stress, Equation 2.13, applicable for the saturated soil [7]. In this approach both the degree of saturation and the suction is neglected. This is in the modelling process done by *ignoring suction* in the calculation settings. When the suction is *not* ignored, Plaxis consider suction and degree of saturation through Bishop's definition of effective stress [11], Equation 2.14 [7]:

$$\sigma' = \sigma - p_{active} \tag{2.13}$$

$$\sigma' = \sigma - p_{active} + \chi(p_{active} - p_{water}) \tag{2.14}$$

in which χ is the effective stress coefficient related to the degree of saturation and usually determined experimentally [34]. This is in Plaxis 2D equal to S_{eff}. This gives that the Bishop's stress is given by Equation 2.15 seen below. For a soil with full saturation the Bishop's stress corresponds to Terzaghi's effective stress [8].

$$\sigma' = \sigma - S_{eff}(p_{steady} + p_{steady}) = \sigma - p_{active} \tag{2.15}$$

Plaxis does not consider the change in unit weight with the degree of saturation. This would be the most accurate, but only the phreatic level is considered [7]. For a fully coupled flow analysis, the unit weight is based on p_{water}, allowing the the phreatic level and thereof the unit weight to change.

Safety Factor Calculation - phi/c Reduction

The safety calculations in Plaxis is performed using the phi/c reduction method. The shear strength parameters, tan ϕ and c, along with the tensile strength are progressively reduced until failure [7]. The safety factor with respect to ϕ and c is increase in a synchronized manner so that $\eta = \eta_\phi = \eta_c$. From this the total multiplier $\sum M_{sf}$, the safety factor, is defined by the Equation 2.16:

$$\sum M_{sf} = \frac{tan\phi_{input}}{tan\phi_{reduced}} = \frac{c_{input}}{c_{reduced}} = \frac{s_{u,input}}{s_{u,reduced}} = \frac{Tensile\ strength_{u,input}}{Tensile\ strength_{u,reduced}} \tag{2.16}$$

meaning the strength reduction required to reach failure is considered the factor of safety.

Soft Soil Model

The Soft Soil model is based on the Modified Cam Clay which is an elastoplastic soil model that is capable of computing nonlinear elasticity and softening/hardening in plastic behaviour [33]. The model is suitable when concerned with fine-grained soil that is normal to slightly over consolidated where a lot of compression can be expected under loading. The failure condition of the model is the Mohr-Coulomb shear and tension failure condition.

The main input parameters for the Soft Soil Model are the modified swelling- and compression index $\lambda*$ and $\kappa*$, which can be found through the oedometer test or empirically estimated through CRS and Triaxial test [33] through Equation 2.17 and Equation 2.18 [51]:

$$\lambda* = \frac{1.1 \cdot \sigma'_{vc}}{M_L} \tag{2.17}$$

$$\kappa* = \frac{2 \cdot \sigma'_V}{M_0} \tag{2.18}$$

$$K_{0NC} = 1 - sin(\phi')\sqrt{OCR} \tag{2.19}$$

Where σ'_{vc} is the vertical component of the pre-consolidation pressure. The other Soft Soil input parameters are the modified Poisson's ratio v_{ur}, modified bulk modulus $K*$, OCR, friction angle ϕ', dilatancy angle ψ , confined modulus M_0 and the stress ratio K_{0NC} from Jaky's formula Equation 2.19 [33]. The parameters are sensitive to changes in POP or OCR, thus determination of the pre-consolidation pressures should be done thoroughly.

3
Method

This project is performed in three phases: literature review, case study and numerical analysis. The case study is separate from the numerical analysis and the results from the phases will be presented and discussed independent of each other. Laboratory work is performed to gain the particle size distribution (PSD) for three samples from the case study sites. The PSD results are used as input for the hydraulic conditions the numerical model. The case study consists of two site visits and discussions with SGI to gain insight about the design choices. The design is compared to best practises found in the literature study after which improvements and challenges are explored. The numerical analysis is focused on the hydraulic effects of vegetation on slope stability and explores the change in failure mechanism caused by these effects in slopes with varying angle. A conceptual mode of the numerical work is presented in Figure 3.1. The change in failure mechanism is related to a factor of safety analysis. The methodology and configuration of the numerical analysis is explained in Section 3.2.

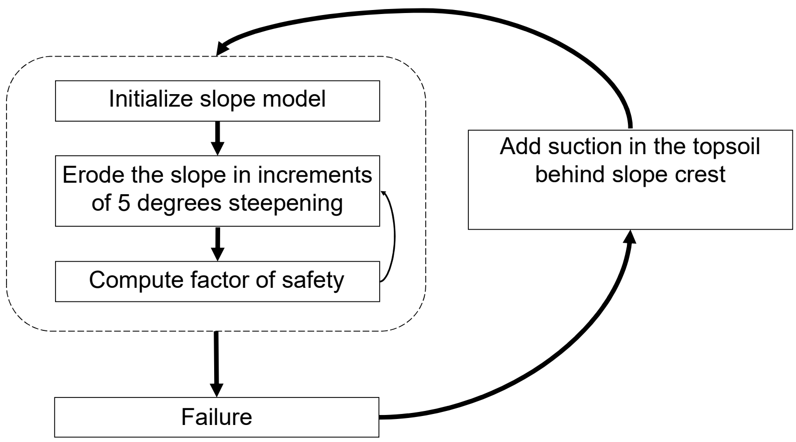

Figure 3.1: Conceptual model of the method concerning Plaxis models.

3.1 Particle Size Distribution Lab Testing

Disturbed top soil samples were collected at Rösbo and four particle size distribution tests were conducted to determine the particle size distribution (PSD) and the classification of the soil. This was used as input parameters for the van Genuchten flow model in Plaxis. The PSD tests were conducted as follows. Water content is

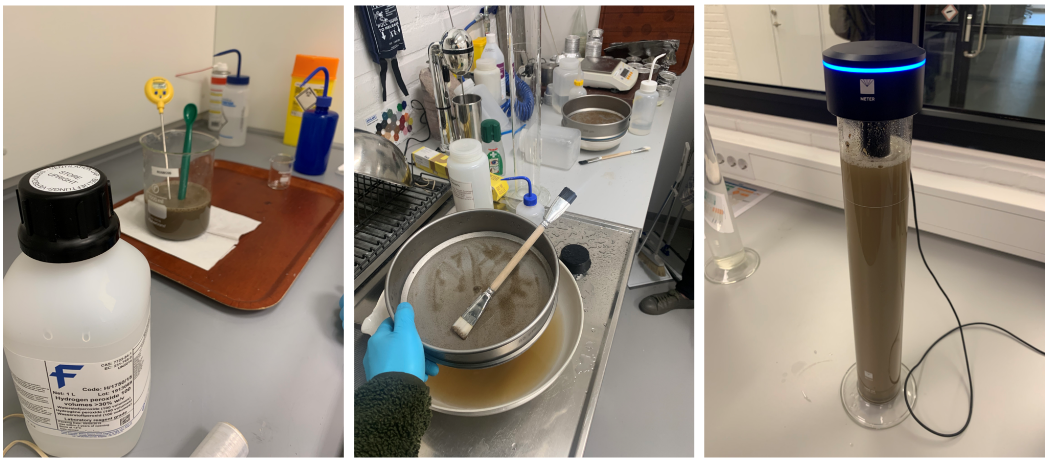

Figure 3.2: Destruction of organics, sieving of sand and the PARIO in action.

measured according to ISO 17892-1:2014, by comparing wet mass to the mass of the same sample under over drying at 110 C°. Following this, the organic content of the dry samples are estimated by loss on ignition according to SS-EN 15935:2021 by burning the samples in a furnace at 550 C°. If the measured percentage weight loss after extended exposure exceeds 3% when compared to the calculated dry mass, destruction of the organic content is required and is conducted by chemical means through addition of hydrogen peroxide. See Figure 3.2.

Once organic content has been removed and the added chemicals separated from the remaining soil mass through centrifuging, a dispersion solution is added to the soil together with distilled and deionised water, to disperse flocks of particles. The soil-dispersion solution is mixed by mechanical means and kept in motion for about 12 hours (SS-ISO 11277:2020). At this point the sample is ready for sedimentation testing, which is a method of PSD testing where the temporal density change in the fluid is used to find particle diameter distribution. This is only done for the fine soil, everything larger than 2 mm has been sieved out and measured, this is the coarse fraction of the sample. A Meter PARIO automatic pressure recording device was used to record, calculate and plot the results, based on Stoke's law [52].

The sample is then wet sieved through 63 to 0.063 *mm* sieves to find the sand fractions. At this point the sedimentation analysis and the sieve analysis can be combined for a complete PSD curve and soil classification.

3.2 Numerical Modelling

As described in Chapter 2.2, vegetation contribute to numerous effects on both erosion and the stability of a slope. The focus of this study is the hydraulic effects that vegetation has on a slope through negative pore pressures induced in the shallow soil layers behind the slope crest. The model aims to investigate how the global stability of a slope is affected by this suction. Simply described, a bare slope without suction is created and is iteratively steepened until failure. Factor of safety, mean effective stress and shear strain is noted for each slope angle. Following this, constant head boundaries of negative pore pressure proportional to those induced by evapotranspiration are introduced in to the model. The amount of suction is based on measured levels in previous studies, see Section 2.2. The steepening iterations are repeated and the results are compared.

As there is a lack of input data from the case study sites, the numerical analysis will cover a virtual idealised slope based on data from different locations. PSD from the case study site is used for material flow parameters, but the main soil data is gathered from two boreholes on the east side of Göta älv at a site close to road E45. In addition to this, values for unit weight and Poisson's ratio were based on [33]. Initial void ratio was assumed to 0.5 and change in permeability to 1.0.

Model Configuration

In the Plaxis model, a fully coupled flow-deformation analysis is performed; meaning that suction, unsaturated behaviour and reduction in hydraulic conductivity in the zone above the groundwater table is accounted for. Constant head boundaries are applied to achieve various levels of suction in the upper part of the slope. Three boundaries are introduced into the model, presented in Table 3.1 and Table 3.2 where depth and head boundary is presented. Each boundary stretch horizontally 9 m at the surface, from the slope crest and backwards.

Two different root architectures are explored, a plant species with exponentially decaying root distribution and one with parabolic distribution. The exponentially decaying distribution will reach peak suction at the surface, $depth = 0$, and the parabolic distribution reaches peak suction at half the root depth, $depth = \frac{root\ depth}{2}$. No plants are assumed to grow on the eroding slope surface, vegetation is applied until the crest of the slope but no further. The maximum root depth is assumed to 0.4 meters and roots are allowed to grow to half that distance in the horizontal direction past the vegetation boundary, represented by the middle boundary reaching that distance. No mechanical effects from vegetation are considered in the analysis. The modelling process in Plaxis is described in Table 3.3.

Table 3.1: Constant head boundary for exponentially decaying root distribution.

Depth [m]	**High suction [m]**	**Medium suction [m]**	**Low suction [m]**
0	-20	-10	-2
0.2	-10	-5	-1
0.4	-5	-2.5	-0.5

Table 3.2: Constant head boundaries for parabolic root distribution.

Depth [m]	**High suction [m]**	**Medium suction [m]**	**Low suction [m]**
0	-10	-5	-1
0.2	-20	-10	-2
0.4	-5	-2.5	-0.5

Table 3.3: Modelling process in Plaxis.

Model stage	Description	Calculation type
1	A horizontal plane is set up in Plaxis to initialize the stress conditions of the model	K0 procedure
2	The river bank and bed geometry is created by deactivating horizontal slices, creating the model slope	Plastic
3	Consolidation until 90% degree of consolidation, resetting small strains & displacements, updating mesh	Consolidation
4	Introduction of constant head boundaries and final ground water conditions are set, 500 days time interval to normalize pore water pressures	Fully coupled flow-deformation
5	Factor of safety is calculated	Safety analysis
6	A slice is deactivated to create a steeper slope	Fully coupled flow-deformation
7	Stages 5 - 6 are repeated for 10 slope angles, in increments of 5°	-
8	Stages 4 - 7 are repeated for low, medium and high constant head boundaries, and a reference slope with no constant head boundaries	-

Geometry

The slope is set up using a basic geometry of a slope with an inclination of 1:3 corresponding to a slope angle of 18.43° with one uniform clay layer to simplify the model. The ground level behind the crest is set to level +2 and the groundwater level is set to a level of +1 behind the slope crest, this is kept constant through the erosion process. The water level of the river is set to level -1. In the iterative process of erosion the slope is steepened in steps of 5 degrees. Figure 3.3 shows the initial geometry of the 18.43° slope.

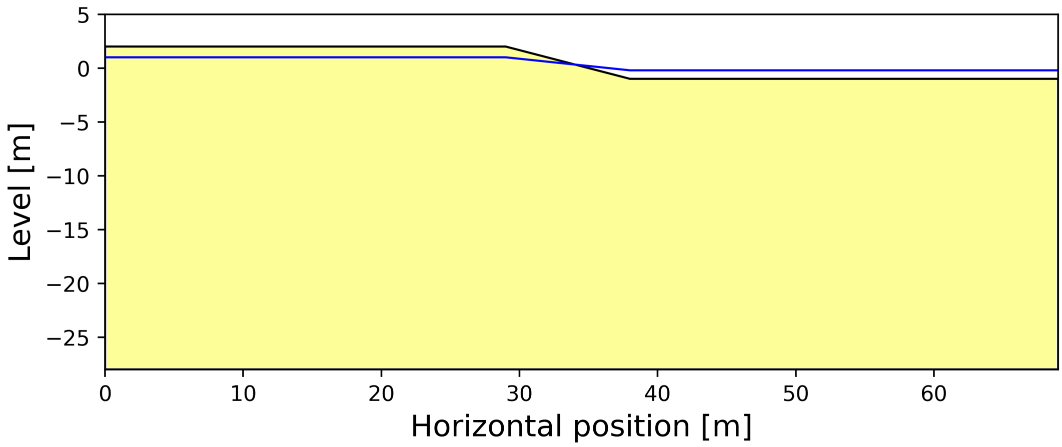

Figure 3.3: Initial geometry of the slope, groundwater table in blue.

Derivation of Material Parameters

The numerical analysis covers a virtual slope based on data from different locations. The main soil data is gathered from two boreholes, FB2201 and FB2202, on the east side of Göta älv at a site close to road E45. As input for the model, average values from the CRS tests of samples collected at 12 meter depth for the two boreholes is used.

The CRS parameters chosen are verified through the Plaxis soil test tool, in which the model input parameters replicate the expected virtual lab results which are iteratively curve matched to the actual CRS lab data to ensure parameters have been correctly chosen. The result from the lab test tool is presented in Appendix D, Figure D.2. The final input parameters are presented in Table 3.4. The drainage type of the clay material is set to *undrained A* to account for excess pore water pressures, though for consolidation and fully coupled flow-deformation calculations, Plaxis defaults to the defined material flow parameters. These characteristics are in this model based on the Van Genuchten parameters, which relates to the soil classification gathered from the PSD lab tests.

The final derived parameters for the clay layer can be seen in Table 3.4. The parameters for groundwater flow and permeability can be seen in Table 3.5. The permeability is defined by the van Genuchten model which takes PSD as input. The PSD used was gathered from lab tests on disturbed clay loam samples from the case study site. CRS tests were used for general material model parameters and combining these with flow inputs from a different material becomes a limitation of the model.

Table 3.4: Input parameters in Plaxis, Soft Soil model. A uniform clay loam layer.

Parameter		**Value**
γ_{unsat} $[kN/m^3]$	Unsaturated unit weight	16
γ_{sat} $[kN/m^3]$	Saturated unit weight	16
e_0	Initial void ratio	0.5
$\kappa*$	Modified swelling index	0.25
$\lambda*$	Modified compression index	0.007
c'_{ref}	Effective cohesion	1.5
ϕ' $[°]$	Friction angle	31
ψ $[°]$	Dilatancy angle	0
v'_{ur}	Poisson's ratio for unloading/reloading	0.2
K_0^{nc}	Coefficient of lateral stress in normal consolidation	0.4850
OCR	Over-consolidation ratio	1.0
POP $[kN/m^2]$	Pre overburden pressure	30

Table 3.5: Parameters for groundwater flow, USDA data set and Van Genuchten model is used. The flow parameters, k_x and k_y are obtained from grain size distribution.

Property [unit]		**Value**
Soil type		Clay loam
$< 2\mu m$ [%]	PSD	34.00
$2\mu m - 50\mu m$ [%]	PSD	34.00
$50\mu m - 2mm$ [%]	PSD	32.00
k_x $[m/day]$	Permeability	2.88E-3
k_y $[m/day]$	Permeability	2.88E-3
e_{init}	Initial void ratio	0.5
S_s	1/m	9.492E-6
c_k	Change of permeability	1.0

Mesh Convergence Analysis

A mesh convergence analysis is performed to check the influence of mesh refinement and number of elements on the result. This is done by iterative refinement of the mesh, running the calculation and comparing the safety factor for each refinement to the initial case with and without suction. The result from the mesh convergence analysis can be seen in Figure 3.4. From this it can be concluded that the number of elements have limited impact on the safety factor of the slope. But it can be noted that the mesh will impact the result of internal forces in the slope for example the distribution of excess pore pressure, and for this a higher refinement of the mesh might be beneficial.

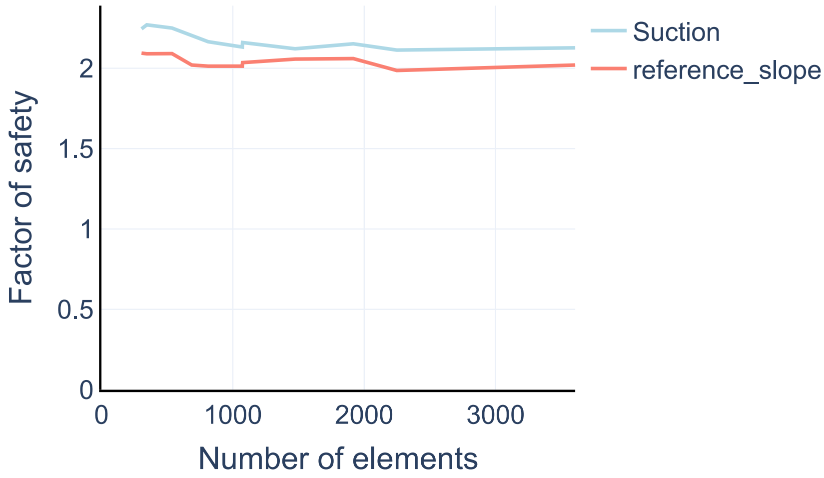

Figure 3.4: Mesh convergence analysis.

Presentation of data

The result from the Plaxis analysis is presented in contour plots created with Python using the packages *Scipy*, *Matplotlib*, *Pandas* and *Numpy*. The irregular grid data from Plaxis was manually exported and linearly interpolated to a grid using Scipy, this data was plotted using the Matplotlib *countourf* function. The main advantage other than the aesthetic gain compared to the standard plots in Plaxis is that several parameters can be presented overlain in the same figure, which enhances comparability. This is especially advantageous in this study where negative pore pressures, which is related to effective stress, is to be compared to failure mechanisms, which is related to shear strain. These parameters presented in the same figure give a much better representation of the interaction between the two than if they were to be presented separately.

4
Results

In this chapter the results the numerical analysis are presented and discussed. Factor of safety analysis and contour plots of slope models displaying mean effective stress and incremental shear strain are presented.

4.1 Numerical analysis

Safety factor analyses were done for eleven slopes with inclinations varying between 18.43 and 68.43 degrees. For every slope angle three levels of suction was tested for two suction distribution patterns, totalling seven scenarios for every slope inclination when including the reference slope without suction. The suction distributions are presented in Figures 4.1 and 4.2. These suction distributions are for the 1:3 starting slope angle. The exact boundaries that generate these negative pore pressures are presented in Table 3.1 and 3.2. These are kept constant during slope steepening. The results from the exponentially decaying distribution pattern is presented in Figure 4.3, the results from the parabolic distribution pattern is presented in Figure 4.4. To compare the difference between suction distributions, factor of safety increase from the reference slope for different slope angles, for both distribution patters, is presented in Figure 4.5.

Following the safety analysis the results are studied in detail, investigating the mechanisms that affect slope stability using the distribution of mean effective stress and the incremental plastic strain to compare the evolution of failure planes. Four plots are presented for each inclination, one for the reference case and one corresponding to the low, medium and high constant head boundary respectively, see Table 3.1. The four plots are presented until failure of the reference slope, and the plots of higher suction slopes at steeper angles can be found in Appendix F. Notice the change in shear band geometry for varying levels of suction. As can be seen in figure 4.5, there is barley a difference in factor of safety between the exponentially decaying suction distribution and the parabolic distribution. A very slight increase in factor of safety for the deeper seated peak suction modelled in the parabolic distribution can be seen, which is consistent for all levels of suction and most inclinations. This difference is negligible however, and thus only the exponentially decaying case is presented here, which is more representative of the shallow root depth modelled.

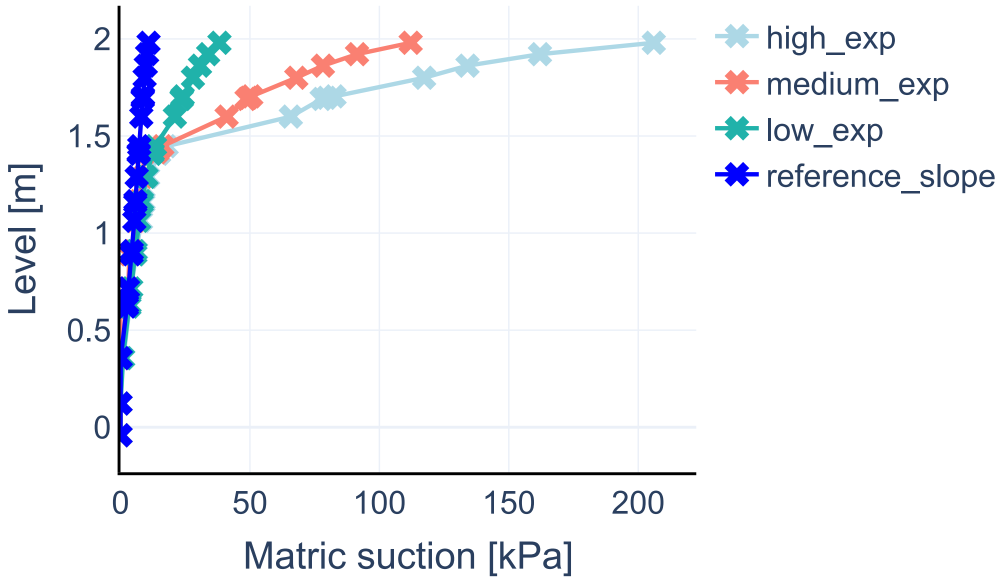

Figure 4.1: Exponentially decaying suction distribution

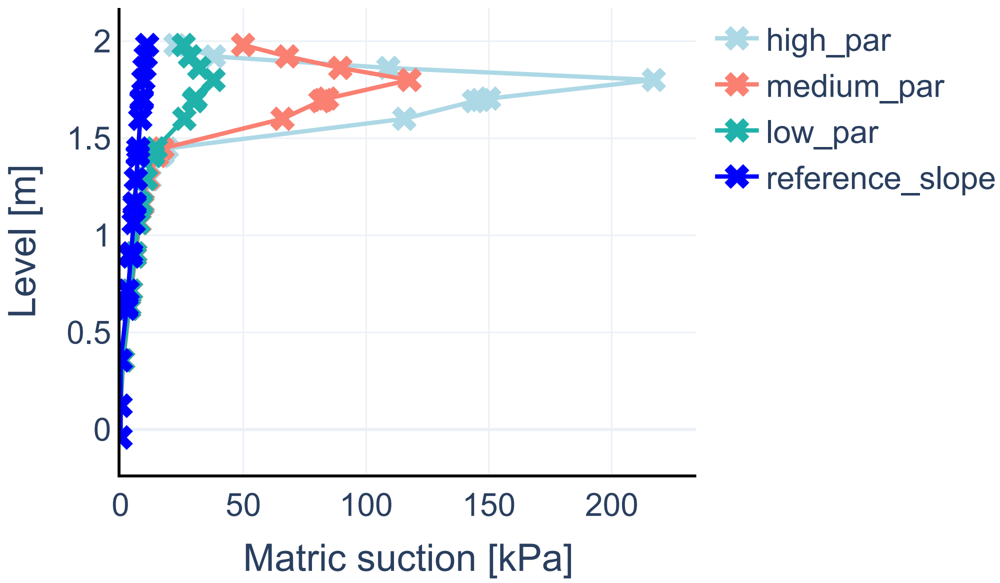

Figure 4.2: Parabolic suction distribution

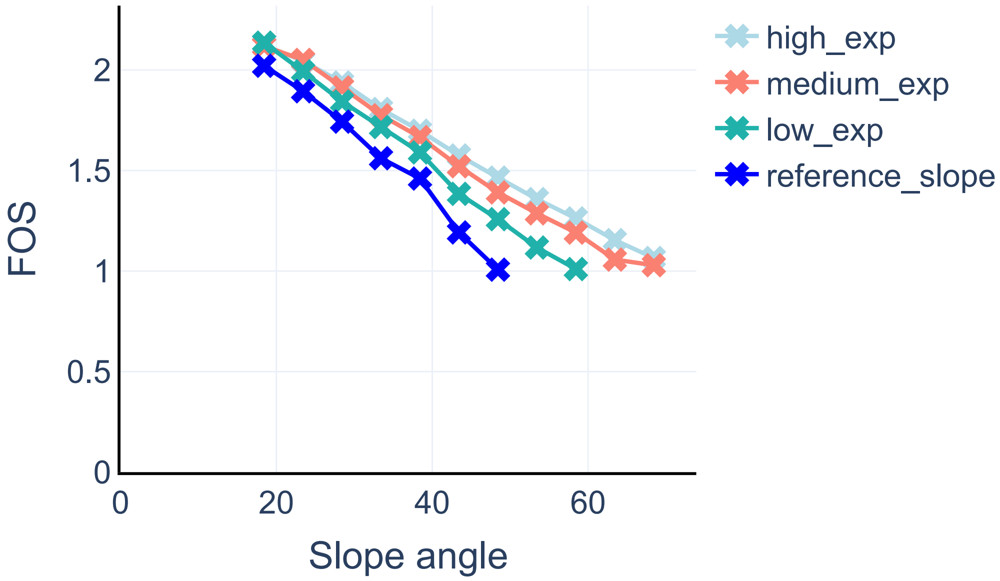

Figure 4.3: Factor of safety vs. slope angle for a exponentially decaying suction distribution.

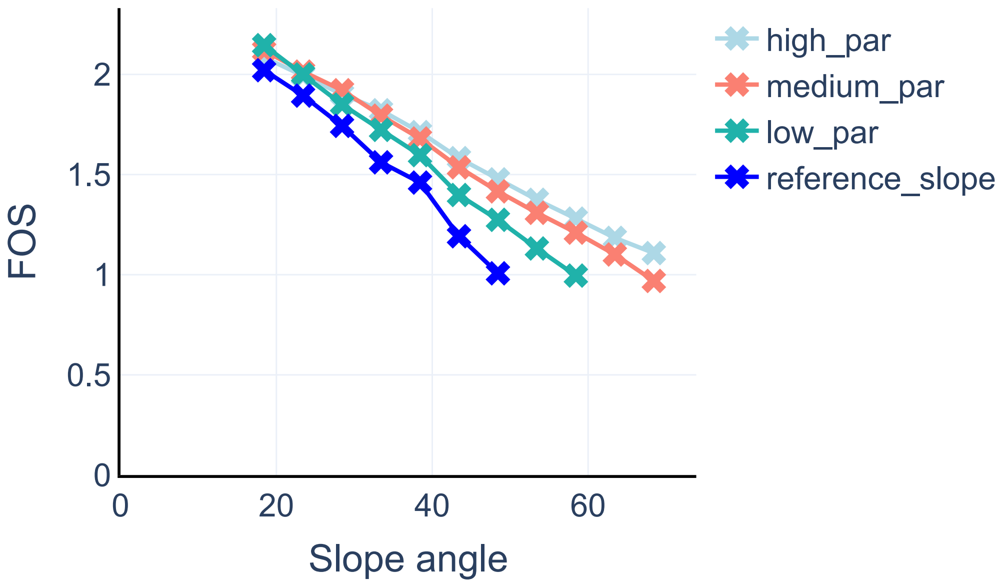

Figure 4.4: Factor of safety vs. slope angle for a parabolic suction distribution.

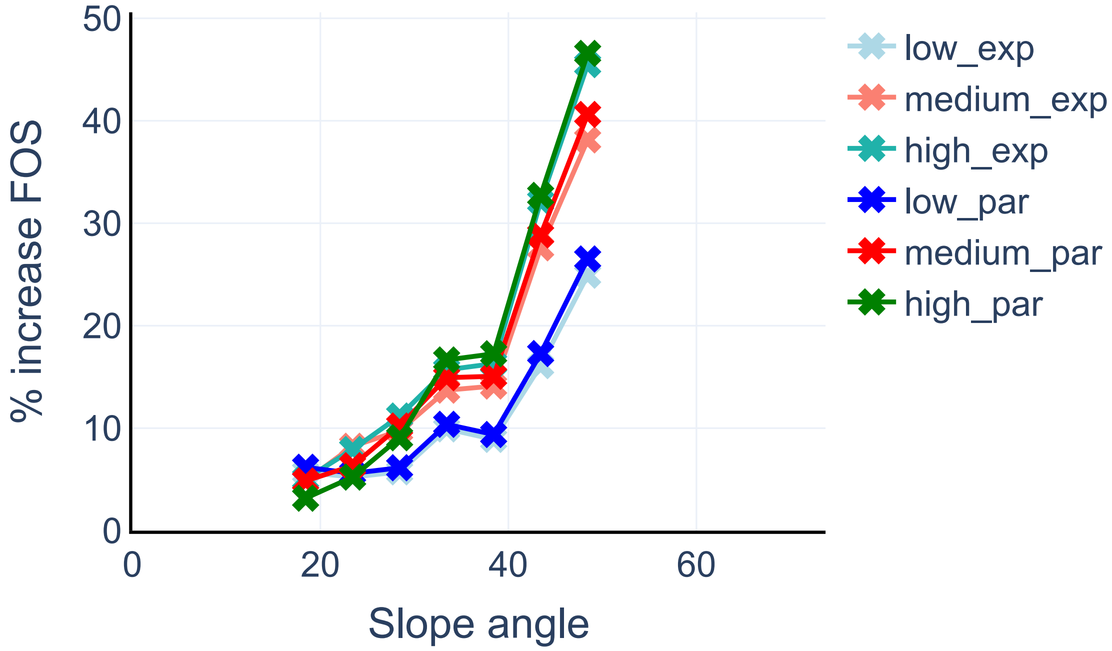

Figure 4.5: Factor of safety increase as function of slope angle, for several suction scenarios.

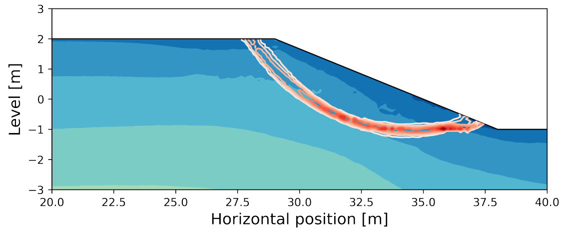

(a) No head boundary

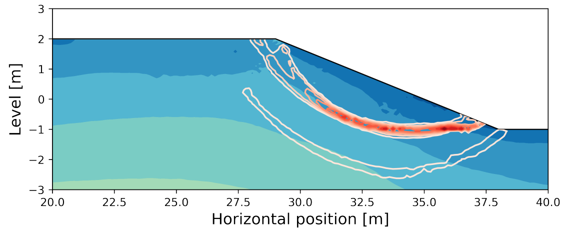

(b) Low head boundary

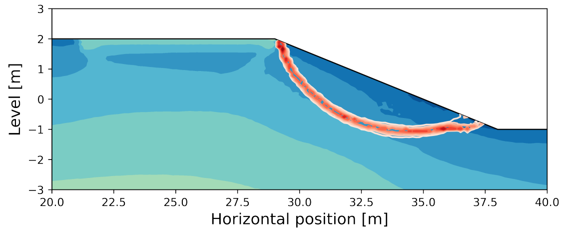

(c) Medium head boundary

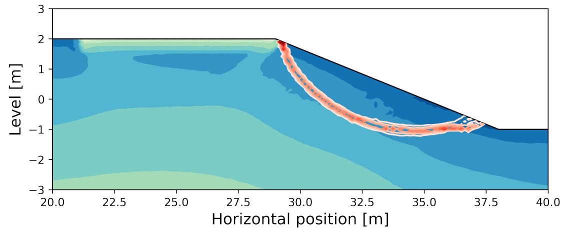

(d) High head boundary

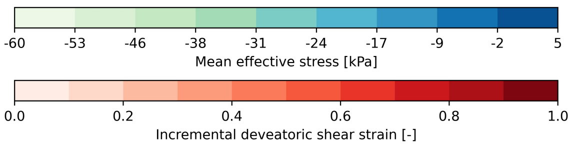

(e) Colorbar for contour plots

Figure 4.6: Results for slope angle 18.43°.

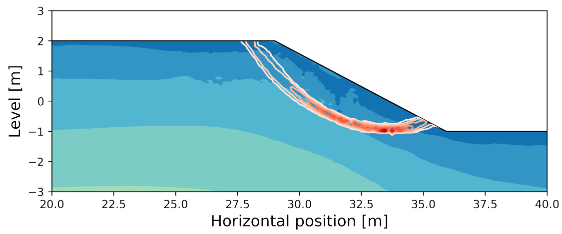

(a) No head boundary

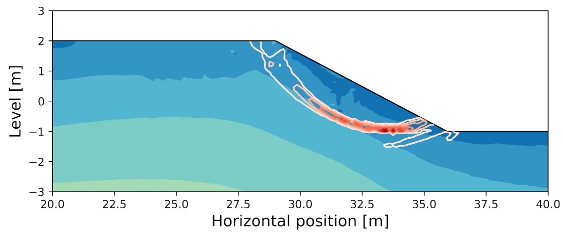

(b) Low head boundary

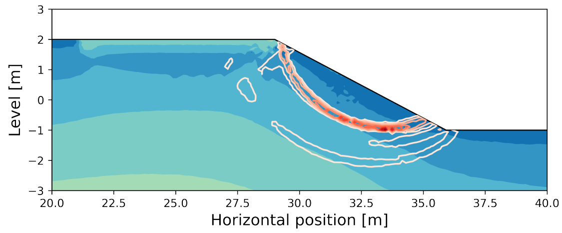

(c) Medium head boundary

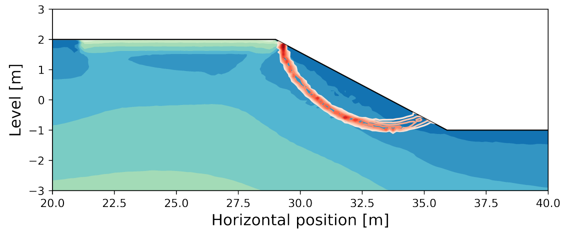

(d) High head boundary

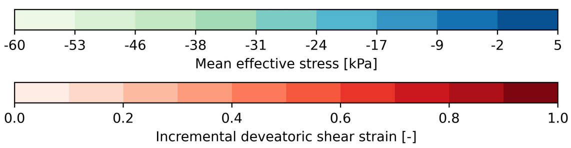

(e) Colorbar for contour plots

Figure 4.7: Results for slope angle 23.43°.

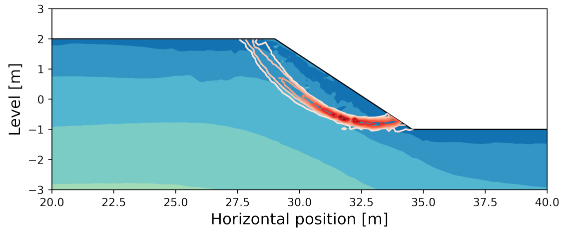

(a) No head boundary

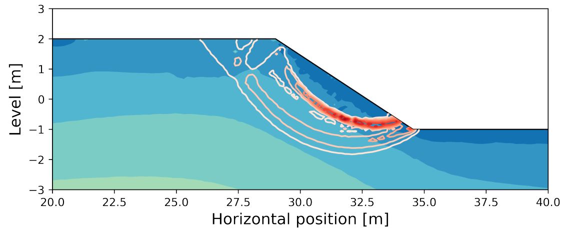

(b) Low head boundary

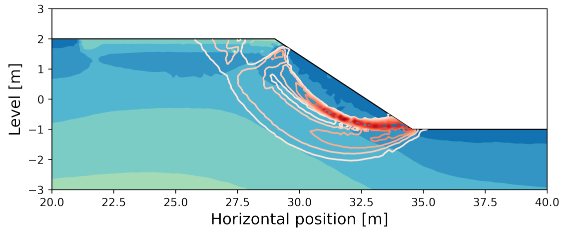

(c) Medium head boundary

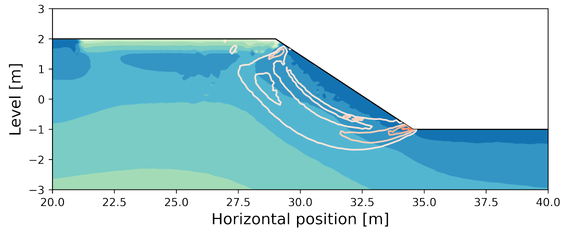

(d) High head boundary

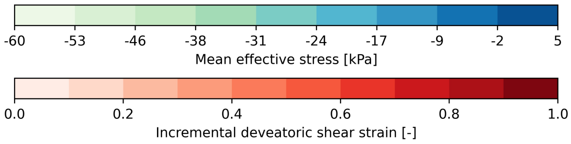

(e) Colorbar for contour plots

Figure 4.8: Results for slope angle 28.43°.

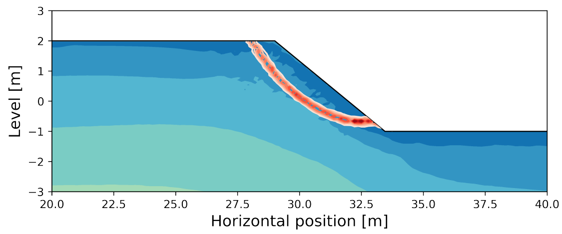

(a) No head boundary

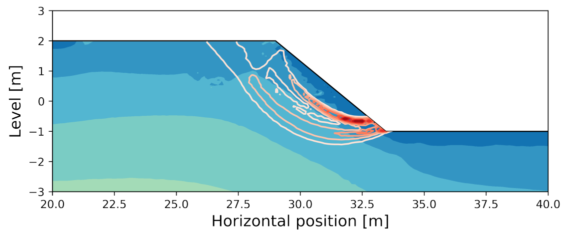

(b) Low head boundary

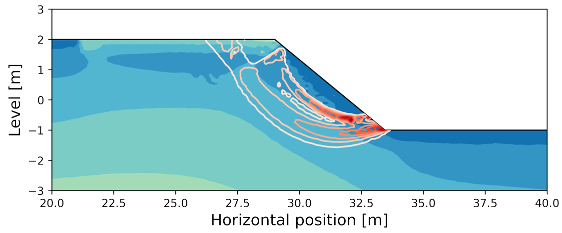

(c) Medium head boundary

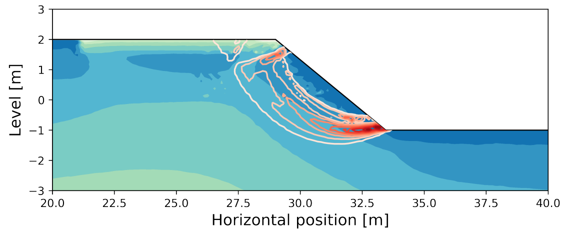

(d) High head boundary

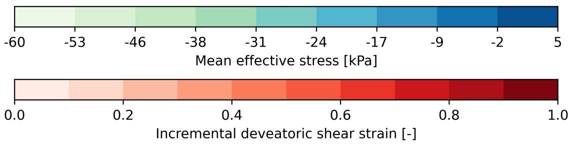

(e) Colorbar for contour plots

Figure 4.9: Results for slope angle 33.43°.

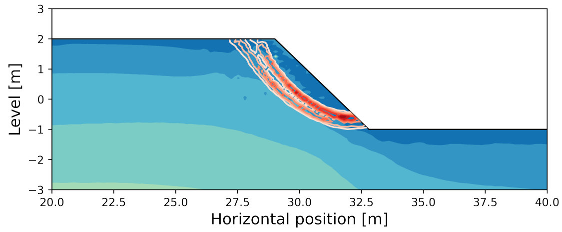

(a) No head boundary

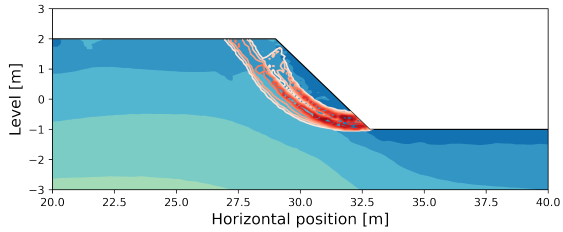

(b) Low head boundary

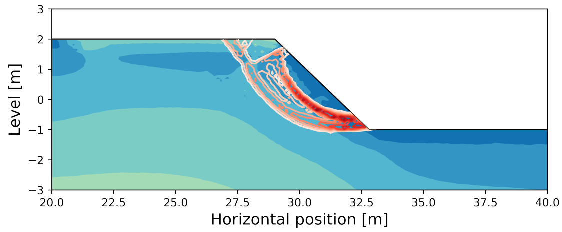

(c) Medium head boundary

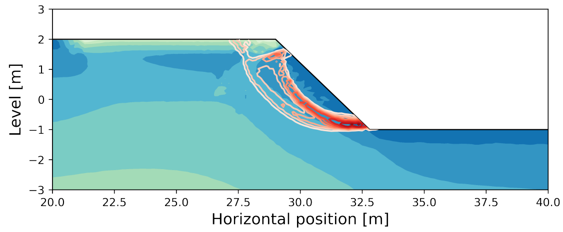

(d) High head boundary

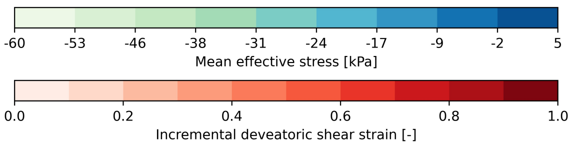

(e) Colorbar for contour plots

Figure 4.10: Results for slope angle 38.43°.

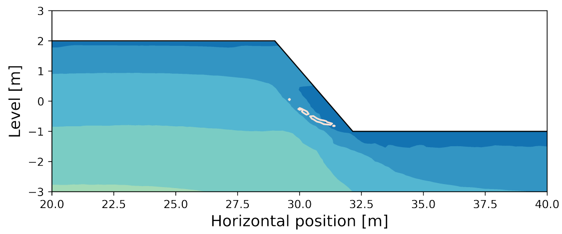

(a) No head boundary

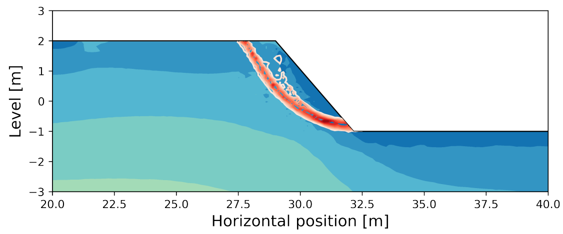

(b) Low head boundary

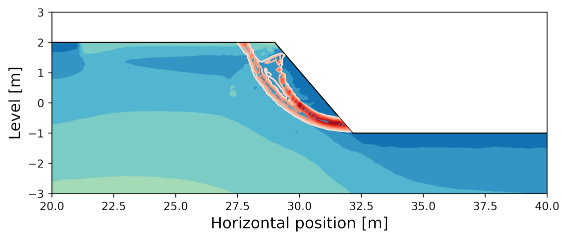

(c) Medium head boundary

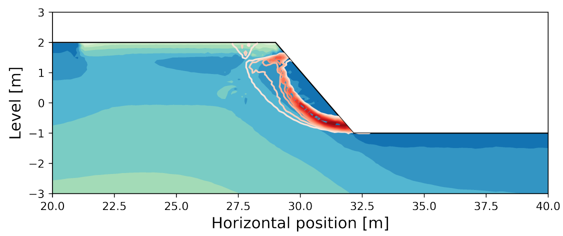

(d) High head boundary

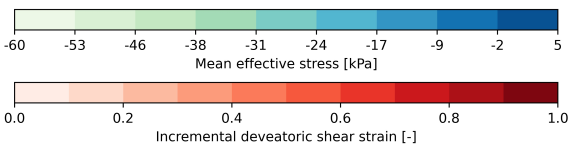

(e) Colorbar for contour plots

Figure 4.11: Results for slope angle 43.43°.

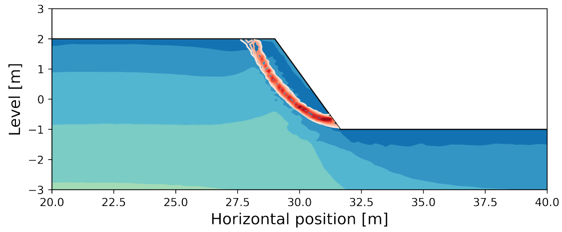

(a) No head boundary

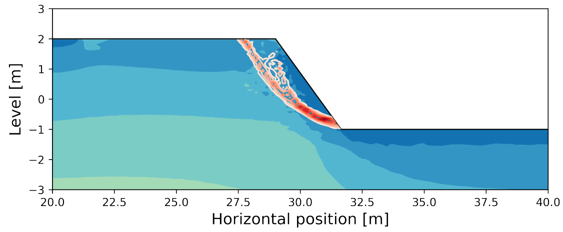

(b) Low head boundary

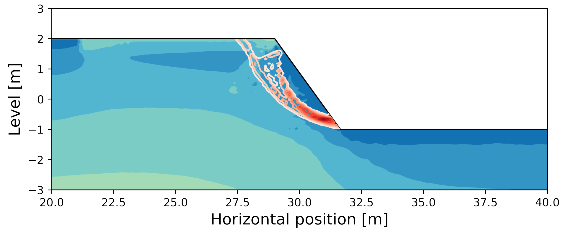

(c) Medium head boundary

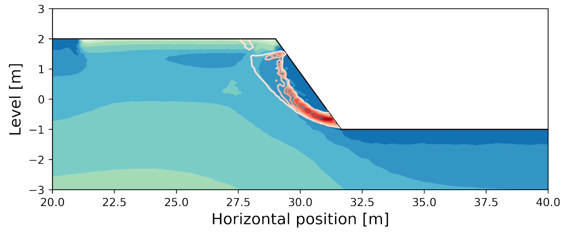

(d) High head boundary

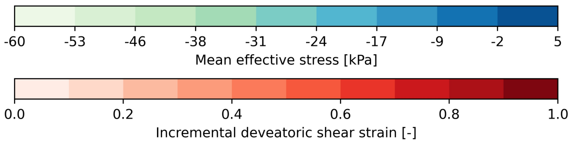

(e) Colorbar for contour plots

Figure 4.12: Results for slope angle 48.43°.

4.2 Interpretation of numerical analysis

Suction has a substantial influence on shear band development and slope stability. This is evident despite the constant head boundaries being limited to the area behind the slope crest and a shallow modelled root depth. Even for low levels of suction a very noticeable change in the failure mode can be seen, shear bands change from being well-defined to scattered into multiple potential slip surfaces. The diffusion of shear bands is most noticeable for low to moderate slope angles - the multiple shear bands coalesce into one for steep angles and high levels of suction. When shear bands fully transition to a new well defined position, the band is shorter and shallower when compared to the reference slope as shear deformations are developing in the soil zone without high negative pore pressures. If the shear bands fail to reach the surface this would likely cause a reduction of the risk of global slope failure, a suggestion that is emphasised by the observed increase in factor of safety for these slopes.

Changes in failure mechanisms are clear from the suction distributions studied and likely these changes would be more pronounced in a model where suction is present on the slope surface as well. Such a model would better represent a functioning NBS as vegetation often is present on these slopes, but to study how the soil-suction response in progressively eroding slope behaves it was deemed reasonable to keep the slope itself clear in this study. The difference between factors of safety for the parabolic and exponential root distribution was found to have very limited impact on the slope stability. The authors have a suspicion that the high ground water table modelled is the root cause for the similar results. The shallow depth of the unsaturated zone leads to relatively small depth at which suction is present. This combined with a root depth of 0.4 meters leads to only very slight differences in pore pressure distribution in the unsaturated zone. A slope with lower water table and larger root depth may experience larger differences in stability attributable to root spatial distribution than what was measured in this study.

Results presented in this paper show that even low levels of suction present in topsoil can have a substantial effect on failure patterns and positive impact on stability. The low levels of suction studied are below what has been found in vegetated slopes in previous studies. The low suction modelled peaks at 42 kPa, compared to e.g. 67 kPa measured by [48] for a tree slope and 50 kPa for a grass slope. This means reaching at least these pore pressures in an actual NBS slope is realistic, even higher values than those measured by [48] are feasible in a combined tree/grass slope as concluded by [49]. That is with one caveat however, and that is assuming favourable soil moisture content and precipitation patterns. That is also assuming a climate and season when vegetation is bearing leaves as evapotranspiration in another case is minimal or non-existent. These caveats pose a serious limitation to the idea that suction can be considered in the design of slopes. It may be suggested that suction induced by vegetation reaches peak levels during conditions critical to slope stability, such as during rain-storms which would mean that considering suction would be appropriate but more clarity regarding patterns of suction variations and the interaction with driving factors of landslides is needed.

When running the numerical analysis some problems attributed to the mesh, the applied head boundaries and the polygons of the eroding slope occurred. High localized pore pressures and numerical divergence errors in some iterations of the model are examples of this. Numerical issues such as these should be considered more carefully in future studies. If further studies were to be conducted the mesh could be analysed further to be able to reach a solution without any locked in pore pressures .

Ideally a separate model for every erosion step should be created to ensure good mesh quality, but as over 30 models would have had to be created this method was not deemed feasible for the project as the risk of model settings discrepancies posed a higher risk of unreliable results in the time frame of the analysis, than numerical noise. It is possible to script this process in Python, which is advisable in future studies covering a similar number of scenarios as this study.

Further studies

The analysis in this study has purposely neglected mechanical impact of roots, which often is the only mechanism analysed when predicting impact of vegetation on slope stability. As this study has shown suction can have a meaningful impact on slope stability, especially in a slope approaching its critical angle. A reason hydraulic effects are often ignored may be the large variations in suction levels that are observed in a vegetated soil. These variations would make it difficult to incorporate hydraulic effects into the design of slopes, but a better understanding of suction variations and how conditions governing these variations may impact slope stability should be the next step in creating a framework of NBS design which considers all aspects of slope-vegetation interaction. When a greater understanding of the interplay of environment, vegetation and slope is reached, a comprehensive combined analysis of mechanical and hydraulic effects of vegetation that considers this interplay should be the next step towards developing a full-scale NBS design practise.

Further studies are needed regarding the implementation of NBS for erosion mitigation in Sweden. In an international perspective there are more well documented studies and guidelines, but geotechnical and hydrological conditions vary greatly as well as available vegetation. There is a need to conduct well documented case studies to be able to create Swedish guidelines in which the NBS implemented by SGI is a first step.

It would be useful to conduct a similar study as the one presented here but incorporated a complete set of input data from a case study site to study how this influence the results. This would be interesting to verify against a real slope for further verification. A look at shear band evolution in a slope with vegetation on the slope face, as opposed to one without as was studied in this paper, may help give a more realistic view of suction effects in a functioning NBS.

5
Case study

The case study consists of four nature-based solutions (NBS) installed by SGI along Göta älv in late 2021. In the following chapter the local conditions of Göta älv, the case study site and the construction of the NBS is described and discussed.

5.1 Göta älv

Göta älv is the largest river in Sweden measured by drainage basin, length and average water flow [61]. Its catchment area covers approximately 50 000 km^2, which about equals to 10% of the area of Sweden. The catchment area starts in the mountainous area far north of lake Vänern and includes parts of the Norwegian highlands [21]. The water runs south through a network of streams and rivers into Vänern before it drains into what is commonly called Göta älv, running south-west until it splits into two segments that eventually reach the ocean Kattegatt. The total combined discharge into Kattegatt of the two segments is about 565 m^3/s, which is the highest average estuary discharge of rivers in Sweden [61], although rivers located further north have more extreme spring flows.

The river is of large importance in regard to societal utility, as it is used as a fresh-water source, for transportation and hydropower [21], generating around 5% of the total energy produced in Sweden [56]. The hydropower means that water levels are highly regulated, which increases the risk of erosion along the riverbanks. The harbour of Gothenburg, located in the estuary of the southern segment is the largest in Sweden. Göta älv is an important transport route, approximately 2000 transport vessels pass the bridge Hisingsbron annually, and 1300 pass the bridge near Trollhättan, located close to lake Vänern [29].

The NBS constructed by SGI are situated on the floodplains of Göta älv, south of Kungälv after the segmentation on the western bank. The approximate location of the NBS site can be seen in Figure 5.1.

Geological and geotechnical conditions

The river and surrounding area is mainly made up of glacial clay, with layers of post-glacial clay and small amounts of sand and gravel [56]. The soil depth is generally large, varying between 20 and 100 meters. Very sensitive quick clay is present at some stretches of the river and the average undrained shear strength of the soil is generally low [56]. The river valley of Göta älv is the result of a large fault running from Vänern southward past Gothenburg, and the bedrock consist mainly of gneiss

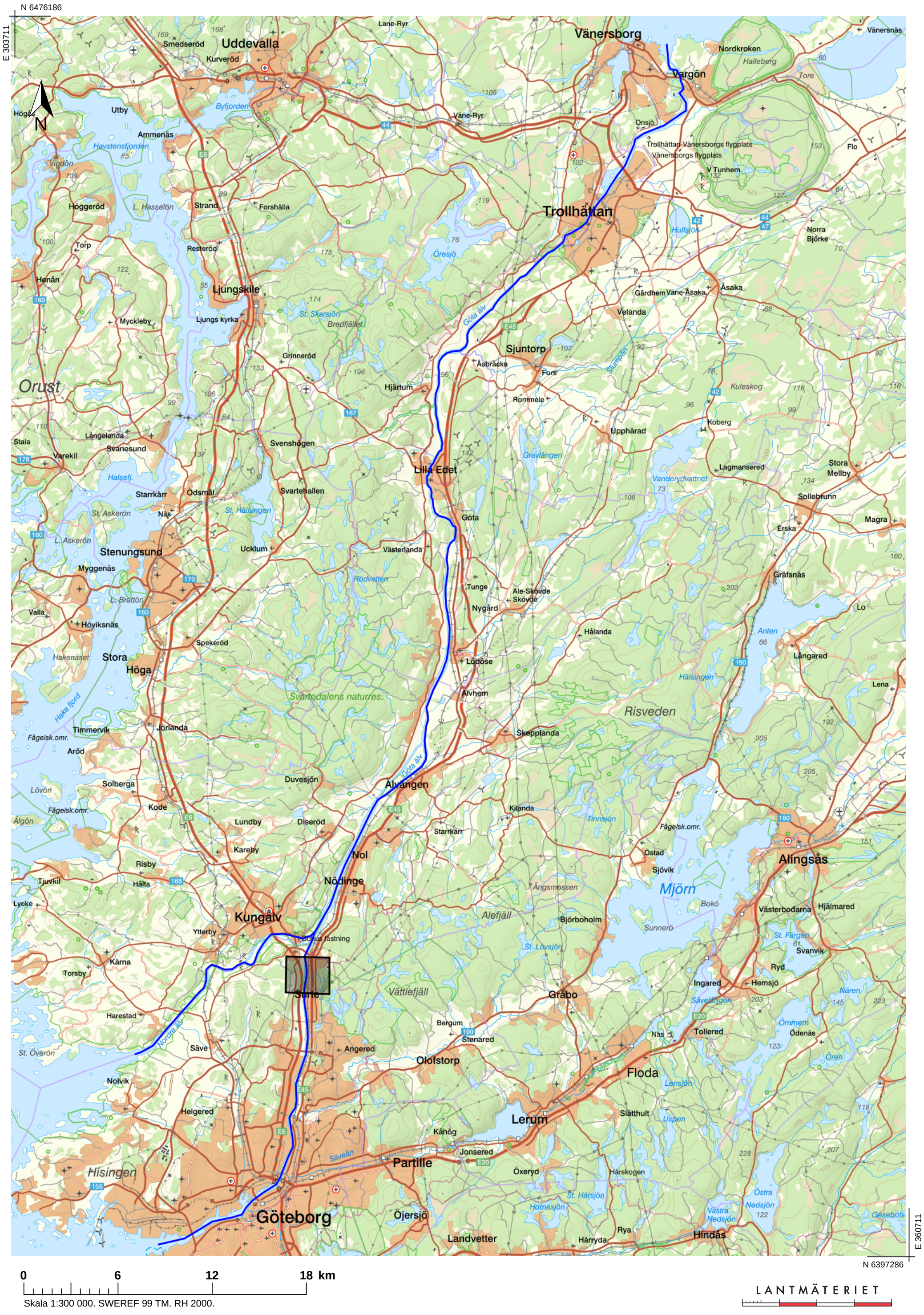

Figure 5.1: Overview of Göta älv, shown as a blue line. Approximate location of NBS site is marked with black square, south of river segmentation. © Lantmäteriet.

and diabase that is highly fractured

These geotechnical conditions have led to several landslides throughout history, resulting in the loss of life and large economic damage in multiple cases. The most extreme case dating back to 1648 when a massive landslide caused the death of at least 85 people. A more recent example is the 1958 slide in Göta, south of Lilla Edet, when an entire field and part of an industrial complex slid into Göta älv, resulting in the death of three people [56]. In many of the landslides recorded in the Göta älv valley, quick clay is a determining reason for the soil stability failure, and erosion of the river is known to be a driving factor in initiating landslides in the area [56].

In previous studies of Göta älv there have been attempts to determine the critical bed shear stress using different types of tests and samples from the river. Although somewhat scattered results, the critical bed shear stress is estimated to be approximately 0.5 Pa [57]. This could be considered as a general value for the river, but more investigations is needed to be able to determine any site specific values.

5.2 Site descriptions

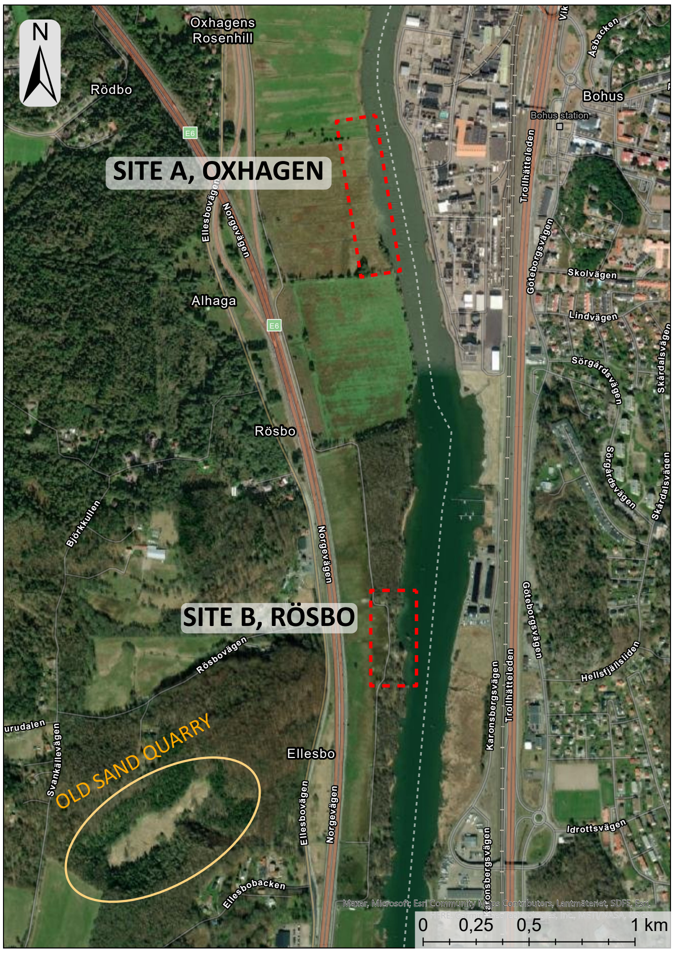

Figure 5.2: Overview of the sites, location marked by red. Old sand quarry in south west, marked by yellow. Lantmäteriet ©.

The four NBS are constructed at two sites, Oxhagen and Rösbo, south of Jordfallsbron on the west side of Göta älv. See Figure 5.2. Both sites previously lacked protection against erosion. The aim with these solutions is to limit the ship wave impact to allow vegetation to take root on the riverbank that today is experiencing on-going erosion and frequent mass movement. This vegetation will then act as further prevention against erosion.

Site A - Oxhagen

Site A is located around 500 m south of Jordfallsbron. From historical aerial photographs it can be concluded that the shoreline at the site has retreated approximately 10-20 meters since 1960. Historical photos of the site can be seen in Appendix A. This could be due to different reasons, man-made or natural, but likely the main cause is erosion of the riverbank.

The area is today a nature reserve [80] and consists of a flat open field with a grassy surface. Small streams of water cross the area from the road in the west reaching the river in the east. The soil consists of a silty clay and overlaying old filing material with mixed content. The soil depth is likely large, 20 - 30 m according to SGUs soil depth map [67]. When site visits were conducted active erosion could be seen, resulting in the loosening of larger chunks of soil.

NBS A1 - Coir Rolls Pressed Against Riverbank

Figure 5.3: Photo of NBS A1 from site visit 2022-01-26.

NBS type A1 consists of coir rolls pressed against the top of the riverbank by wooden piles at an angle of approximately 26 degrees. The schematic design of the solution can be seen in Figure 5.7. The coir rolls are installed so that the upper edge is slightly above the mean water level in the river. It can be noted that the waves from passing ship traffic will rise significantly higher than this level, leaving the protection from the coir rolls limited. The loss of material into the river should however be somewhat limited, at least initially, as material gets stuck between the coir rolls and the slope.

NBS A2 - Floating Coir Rolls

Figure 5.4: Photo of NBS A2 from site visit 2022-01-26.

Type A2 consists of coir rolls floating in the water, 0.5 - 2 m from the shoreline. The coir rolls is installed so that the upper edge is at the mean water level of the river. Erosion might still occur behind the protection but the goal is that the material will stay behind the coir rolls and form a new natural slope a lower angle that will allow new vegetation to be established. The schematic design can be seen in figure 5.8. One concern with this solution is that the coir rolls decay at a rather fast rate as it is constantly under water, leaving the mitigation effect limited.

The sustainability of using coir rolls can also be discussed as the material in the coir rolls usually cannot be produced in Sweden and therefore requires long transports.

Site B - Rösbo

Site B, Rösbo, is located south of site A in a section of river where the bank has eroded 40 meters since 1960. The large amount of erosion has led to an asymmetrical river geometry, underwater slope following the west river bank is very gentle with shallow water depth for tens of meters before a steep drop down into the centre of the river. It is the steep, low bank that is retreating and in need of protection. Some 20 meters from the shoreline, in the shallow gentle slope, there are small sediment islands with vegetation clustered where the old shoreline used to be, creating a barrier in front of the bank. The long shallow slope combined with the sediment built up in front of the river bank means that water flow velocity is very low at this site and ship waves are likely the main driver of further erosion. No form of erosion protection was in place before the installation of NBS B1 and B2 at this site while on the east bank, rocks have been placed as erosion protection and this slope is practically unchanged since 1960.

The material at site B is notably around 0.5-1 meters of sand overlaying a loamy clay. This is unusual for the region that is as described dominated by fine-grained clayey material, but in Ellesbo just south west of the site old aerial photos show a sand quarry which is not visible today. The existence of this quarry is confirmed two hydrogeological reports by SGU by published in 2004 and 2009 respectively [36, 37]. The coarse-grained sandy deposition located here is the largest surface deposition of its kind in Gothenburg municipality, but the natural deposition does not reach Göta älv and site B. Ground investigations on the proximity of site B show a thin layer of sand, classified as likely fill material, followed by a deep layer of clay. This information combined with aerial photos from 1960 that show what looks to be a storage area for sand where site B is located lead to the conclusion that the sand layer here is likely not naturally occurring but moved here from the sand quarry in Ellesbo.

There are still a few old sheet pile walls that was erected along the old shoreline though these have mostly been removed, in all likelihood around the time the area became a nature reserve in 1974 [80]. This suggests that material was dug out to be replaced by coarse-grained material - probably for storage purpose - all the way up to the river bank, and when the sheet piles were removed, very erosion susceptible conditions had been created, leading to a large loss of land.

NBS B1 - Stone revel

Figure 5.5: Photo of NBS B1 from site visit 2022-01-26.

The NBS at site B1 consists of an under-water rock barrier designed to breach the water surface during mean water levels. The idea is that this will reduce the wave energy behind the barrier but limiting the impact on the marine life. A reduction in wave energy might allow vegetation to take hold in the foreshore, limiting the rate of erosion in the sandy topsoil. The re-established vegetation is then thought to be the main contributor to soil stabilisation and increased critical shear stress in the bank and bed of the river through root reinforcement and absorption of wave energy.

Figure 5.5 shows the stone barrier during a site visit on 2022-01-26. The barrier is barely visible under the water, and from discussions with SGI it became clear that construction did not follow the design plan, leading to a deeper stone row than planned. Figure 5.9 shows a drawing of the planned design of NBS type B1.

NBS B2 - Piles and Spruce trees

Figure 5.6: Photo of NBS type B2.

NBS type B2 is constructed of wooden piles that fix spruce trees parallel to the mean water surface in a secant line running between two points on the parabolic shoreline with about 15 meter as the maximum distance to the bank. Figure 5.6 shows NBS B2 at a site visit conducted 2022-01-26, the schematic design can be seen in 5.10. It can be noted that the pine trees are visible during a mean and low water level. For higher water levels the trees are not visible, this will likely affect how efficient the mitigation is. The NBS at site B2 is based on the same design idea as B1, that a reduction in wave energy will limit the erosion, making a greater amount of sediment stay behind the barrier. This would allow for vegetation to return to the site and in the long run will this act as a barrier on its own, limiting the negative impact from erosion.

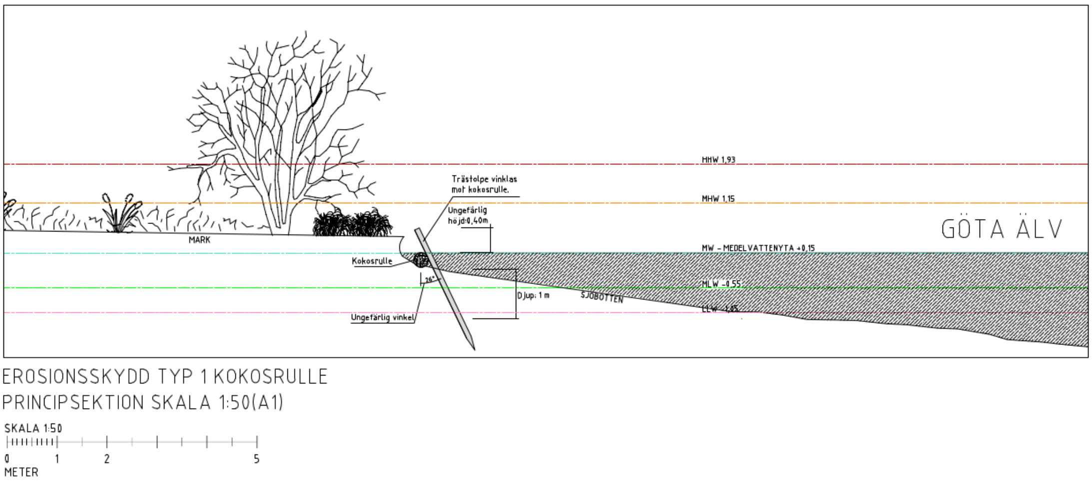

Figure 5.7: Design of A1.

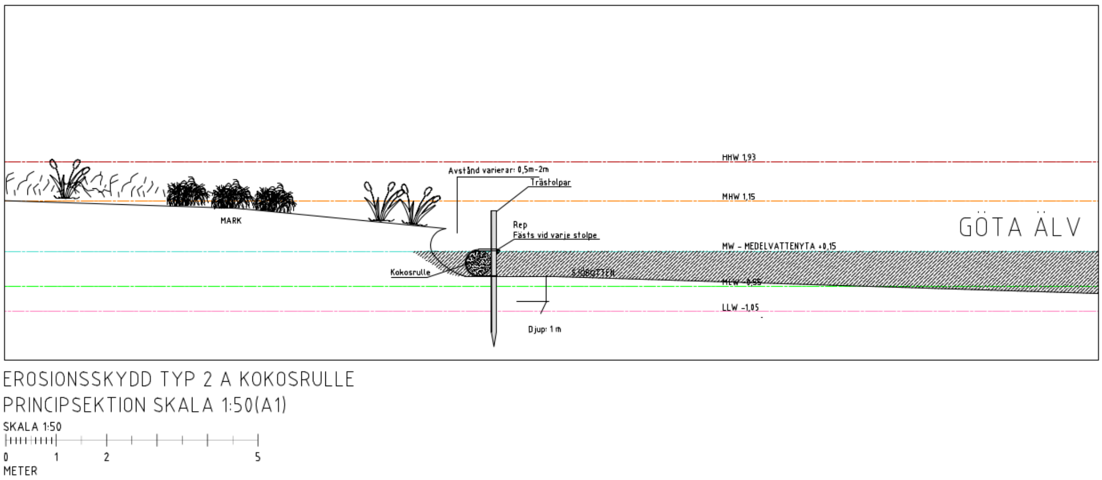

Figure 5.8: Design of A2.

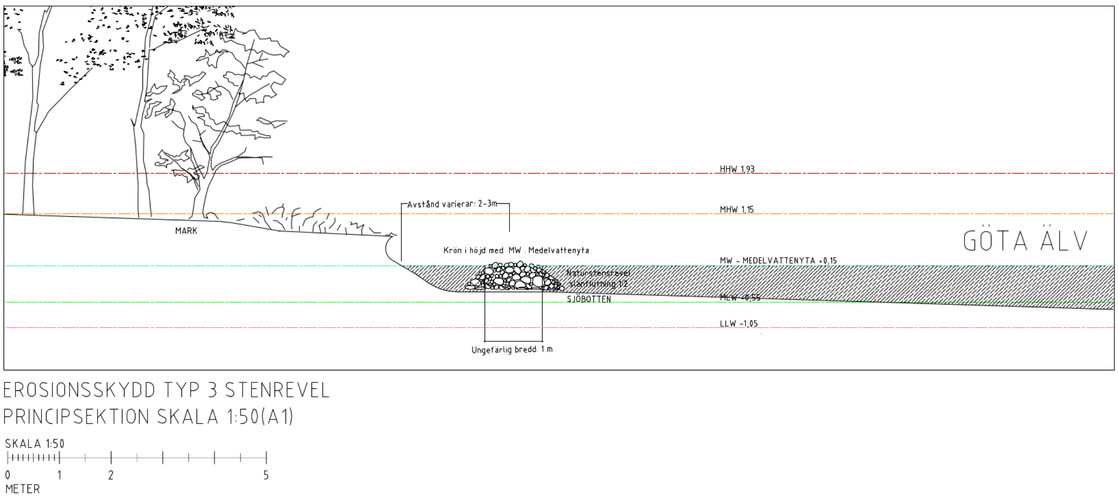

Figure 5.9: Design of B1.

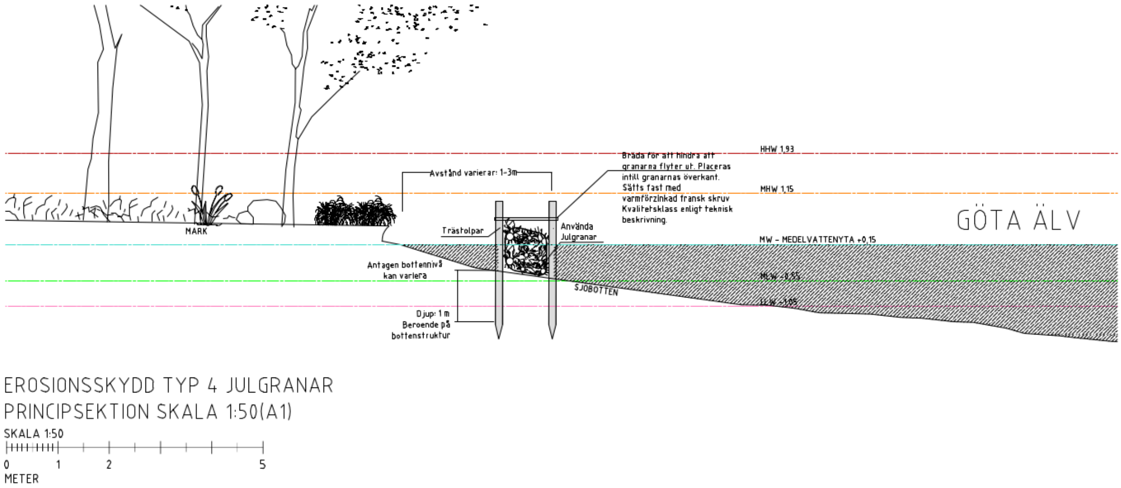

Figure 5.10: Design of B2.

Particle size distribution

The four soil particle distribution tests at Rösbo are presented according to the USDA soil taxonomy system as the software used for analysing the samples is calibrated according to this system. Three of the samples tested came back as variations of sandy loam or loamy sand. These samples were deemed to be unrepresentative for the general area surrounding Göta älv, as this material likely was transported here, see Chapter 5.2. The information is valuable to discuss the effectiveness of the NBS constructed here, but not as input to the more general FEM model. Flow property inputs were instead based on the sample presented in figure 5.11, which was collected at a depth of 1.4 meters in the border of the shallow sand layer and the deep clay layer. The three additional samples are presented in Appendix C.

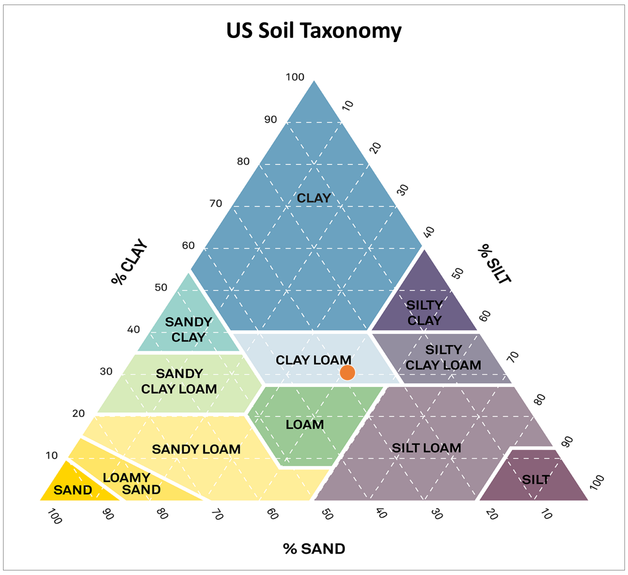

Figure 5.11: Soil PSD in Rösbo, sample 3b. US soil taxonomy.

5.3 Discussion of case study NBS

The NBS constructed by SGI in late 2021 are in their infancy at the time of this thesis. The design philosophy with these solutions is that barriers constructed in the river or on the slopes will lower the amount of wave energy that impact the shoreline. Under these new conditions vegetation should naturally take root without the need for planting or preparing the slope additionally. As the project with the NBS was so recently initialized, construction finished merely months before the start of this thesis, this has not yet taken place. Because of this it is hardly possible to evaluate the effectiveness of the erosion barriers yet. What can be done is to examine the design and construction of the NBS and compare this to current state of the art solutions found through the literature review on the subject. SGI may have a more practical focus in the Göta älv project when compared to this paper, where theoretical knowledge and a perspective based in literature has ruled. Nonetheless a few points are going to be raised as the case study is, perhaps a bit unfairly, compared to findings in the literature review.

Commonly a slope inclination of 1:3 is preferred for most types of NBS, but some sources even suggest an inclination as low as 1:6 [32] for the barrier to work well. Cutting and filling the slopes at both site A and B would likely help vegetation take hold as the part of the slope that is above the mean water surface today is near a vertical inclination (see Figures 5.7, 5.8, 5.9, 5.10) this could prove a hindrance for plants to take hold.

At Rösbo, old trees with large, exposed roots are present in the slope. The soil, uncharacteristically for the area, consists of a very uniform sand that overlay the natural clay beneath. This environment could be susceptible to seepage as this type of coarse, uniform soil has a high hydraulic conductivity. Some of the trees have begun to lose stability in recent times, they are heavily inclined yet without the bent tips that can be seen for trees that have been inclined for a longer time, suggesting still ongoing erosion. Along large roots it is possible that flushing can occur which further accelerates the erosion process. To ease these problems it could be reasonable to mix or cover the existing sand with finer, or coarser, material to create a slope that is less prone to erosion. Considering soil type when designing erosion barriers is important as this will govern the modes of erosion that are dominant, as well as what kind of barriers will be most effective to prevent this. In coarser soil as present in Rösbo, less natural occurring positive hydraulic effects will be seen as suction increases inversely with particle size. But the effect of suction induced from vegetation might be greater. This means that additional measures might have to be taken, a geotextile may for example be beneficial to allow vegetation to take hold under ongoing erosion. This might not be necessary at the site, time will tell.

At Oxhagen the design is made up by wooden stakes and coir rolls that hopefully will retain the eroding material, and by this aiding gravitational forces to create a more gentle slope angle without any cutting or filling. The material is, unlike Rösbo, a uniform clay layer at the top. For the floating coir rolls, type A2, a concern is that they will decay and deteriorate from being below the water level at most times. The mitigation effect from the coir rolls will also be very limited for the waves from passing ships as this significantly raises and lowers the water level momentarily,

Figure 5.12: Erosion behind the bank.

leaving the protection with very limited effect. Behind the floating coir rolls the loosening of chunks of material can already be seen, and the difference from the parts that are unprotected are very limited. This leads us to question the effectiveness of this solution and how long the coir rolls will give any effect. The coir rolls pressed against the shoreline, type A1, might be a more suitable solution. The upper part of the coir rolls is above the water level at a mean water level, therefor they are less likely to rot and deteriorate. A slower rate of erosion can at this point of time be seen compared to the unprotected site.

A concern for the Oxhagen site is the small streams of water that crosses the field from the road in the west, running easterly to the river. This leads to additional surface erosion that might have a negative impact on the implementation of these solutions. Some erosion can be seen behind the installed measure because of this, and may require action to create conditions in which vegetation can thrive. See Figure 5.12 for an example.

The sustainability of using coconut fibres is also an aspect that should be considered. For larger mitigation measures a great amount of material would be needed. The coir rolls are 100 % biodegradable, produced from the husk of coconuts, so that is a positive aspect in the light of ecological sustainability. To reduce transportation distance, a more locally available material might be used instead. The durability of coconut fibre combined with its biodegradability makes it a unique material however, meaning that finding a local replacement might not be straightforward. This would be an interesting area for further studies.

The hydraulic roughness of a channel feature is drastically reduced when plants are submerged. Creating a slope profile where the submersion of vegetation is limited is there for advantageous and this presents a major difficulty in this part of Göta älv, as the water level variations are large both seasonally and cyclically over shorter temporal patterns.

Generally a dense tree cover is to be avoided in a NBS as the shade will limit ground vegetation, which is an important part of a well-functioning nature based erosion protection system. Based on this, a minor concern is that the existing tree cover at site B, which at some stretches is quite dense, may inhibit plant growth on the slope by virtue of restricting sunlight.

Overall the literature that exists on NBS put a heavy focus on species selection. The tensile strength of roots, the root spatial distribution and the amount of induced suction of different species vary greatly and the same slope reinforced with different plants will surely give separate outcomes. Some plants increase the turbulence in the flow which can increase erosion. In the Göta älv NBS project there have been no planting of vegetation, the idea is that natural growth will take place when wave energy is limited. A big advantage of this method is that there is no risk of introducing invasive species to the environment. Another advantage is that if plants do take hold, a less uniform riverbank than a man-made one will emerge. A naturally grown slope will blend into the environment better and may be less monotone, however a non-uniform slope coverage may lead to localized erosion, meaning that some level of vegetation management is likely favourable. For research purpose, the number of uncontrolled variables is large and selecting specific species and plantation patterns would simplify the process of project evaluation.

Further studies are needed regarding the implementation of NBS for erosion mitigation in Sweden. In an international perspective there are more well documented studies and guidelines, but geotechnical and hydrological conditions vary greatly as well as available vegetation. There is a need to conduct well documented case studies to be able to create Swedish guidelines in which the NBS implemented by SGI is a first step.

6

Conclusions

During the literature study several obstacles were found as knowledge of the subject grew. There is a lack of existing comprehensive models to predict erosion, the models that do exist require, for example, bathymetric data as well as very particular soil material data that in no way was available for the site studied. The goal of making calculations to predict erosion was replaced by an aim to link hydraulic impact of vegetation to global slope stability. This was a subject matter still closely related to the initial topic, as well as to the case study, but with the prospect of generating generalized information related to plant - slope interaction.

The model was create with the FEM program Plaxis using the Soft Soil model. Shallow suction was modelled behind the slope crest by creating constant head boundaries of varying intensity and shear band evolution as well as changes in factor of safety is observed. Progressive steepening of the slope was modelled, which is meant to simulate the gradual evolution of an eroding slope that is subject to flow and wave erosion at the toe. Through this, comparisons of failure mechanism evolution at different slope angles was possible. Further studies should investigate how shear band geometry and stability is affected by suction in a local context. Measurements of suction variations in Swedish conditions is also necessary to refine model assumptions.

Parallel to the numerical analysis a more practical phase was undertaken as site visits to the NBS in Göta älv were combined with discussions about design principles and a dive into literature on the topic. Lab work characterizing the PSD of the soil at the site was also done. The main findings of the project summarized below:

- Suction in the topsoil of a slope, even at low magnitudes, noticeably affect the formation of shear bands. There is a diffusion of potential slip surfaces that is most noticeable at moderate slope angles, in which a previously well-defined shear band is scattered into multiple potential failure planes.
- For moderate slope angles between 20° and 40°, the diffusion of failure modes caused by suction in the topsoil is associated with a slight increase in factor of safety, between 5% and 15% depending on slope angle and the magnitude of suction.
- At steep slope angles and high negative pore pressures in the topsoil there is a transition of the shear band into a fairly well-defined new position. During initial conditions the shear band has a large circle sector angle and connects to the ground surface behind the slope crest. The band is well defined in this position. At high suction the shear band bends to a sharper circle sector angle as deformations are avoided in the high suction zone. The result is a shallower

and shorter slip surface that is slightly scattered but with a fairly well defined main direction. This effect is related to a substantial increase in factor of safety, up to 45% for the most steep slope angle studied.

- There are many variables that are difficult to control for and consider in design of NBS. Isolating and gaining an understanding of one at a time is advisable to further gain theoretical understanding which will lead to more robust design principles for Swedish conditions. Further knowledge is needed regarding species selection based on root geometry or other characteristics for local vegetation, seasonal variations in suction and landslide triggers. There is a lack of theoretical knowledge as well as implemented case studies.

Bibliography

[1] alastairdodwell. Preplanted coir rolls, 7 2013. URL https://commons.wikimedia.org/wiki/File:Coir_Rolls.jpg.

[2] Björn Almström. *Nature-based shore protection against ship waves in intra-coastal fairways*. PhD thesis, Lund University Faculty of Engineering, 2022.

[3] J. R.F. Arthur, T. Dunstan, Q. A.J.L. Al-Ani, and A. Assadi. Plastic deformation and failure in granular media. *Géotechnique*, 27(1):53–74, 5 1977. ISSN 0016-8505. doi: 10.1680/GEOT.1977.27.1.53. URL https://www.icevirtuallibrary.com/doi/abs/10.1680/geot.1977.27.1.53.

[4] S Assouline, D Tessier, and A Bruand. A conceptual model of the soil water retention curve. *WATER RESOURCES RESEARCH*, 34(2):223–231, 1998. doi: 10.1029/97WR03039.

[5] Ralph Bagnold, Alger. *An Approach to the Sediment Transport Problem from General Physics*. University of California Berkeley, 10 1966. URL https://books.google.se/books?hl=sv&lr=&id=G096igXqR74C&oi=fnd&pg=PP6&dq=sediment+transport+&ots=C8A6OuXv5s&sig=F9djr0hl8Kww5wviSRWklwlEpIO&redir_esc=y#v=onepage&q=sediment%20transport&f=false.

[6] Gian Battista Bischetti, Enrico Antonio Chiaradia, Thomas Epis, and Emanuele Morlotti. Root cohesion of forest species in the Italian Alps. *Plant Soil*, 324: 71–89, 2009. doi: 10.1007/s11104-009-9941-0.

[7] Bentley. PLAXIS CONNECT Edition V22.01 PLAXIS 2D-Reference Manual, 3 2022.

[8] Bentley. PLAXIS CONNECT Edition V22.01 Scientific Manual, 3 2022.

[9] Bentley. PLAXIS Material Models
}CONNECT Edition V22.01, 2022.

[10] Georgios Birmpilis, Edward Andò, Olga Stamati, Stephen A Hall, Eleni Gerolymatou, and Jelke Dijkstra. Experimental quantification of 3D deformations in sensitive clay during stress-probing. *Géotechnique*, 3 2022. doi: 10.1680/jgeot.21.00114. URL https://doi.org/10.1680/jgeot.21.00114].

[11] A. W. Bishop. The principle of effective stress. *Tekniche Ukeblad*, 39:4–16, 1959.

[12] Albert Brahms. *Anfangsgründe der Deich- und Wasserbaukunst: Band 1*, volume 1. bey Herman Tapper, 1757.

[13] John Bridge. *Rivers and Floodplains.* Blackwell Publishing, Binghamton, 3 2007.

[14] Zhixian Cao, Pender Gareth, and Jian Meng. Explicit Formulation of the Shields Diagram for Incipient Motion of Sediment. *Journal of hydraulic engineering*, 132(10):1097–1099, 2006. doi: 10.1061/ASCE0733-94292006132:101097.

[15] Robert F. Carsel and Rudolph S. Parrish. Developing joint probability distributions of soil water retention characteristics. *Water Resources Research*, 24(5): 755–769, 1988. ISSN 19447973. doi: 10.1029/WR024I005P00755.

[16] N J Coppin, Wardell Armstrong, I G Richards, Richards Moorehead, and Laing Ltd. *Use of vegetation in civil engineering.* CIRCA, 1990. ISBN 0860177114. URL `www.ciria.org`.

[17] Per Danielsson, Johan Kling, Bengt Rydell, and Ramona Kiilsgaard. Naturanpassade erosionsskydd i vattendrag. En förstudie. Technical report, SGI, Linköping, 2016. URL `www.swedgeo.se`.

[18] Frédéric Danjon, David H. Barker, Michael Drexhage, and Alexia Stokes. Using Three-dimensional Plant Root Architecture in Models of Shallow-slope Stability. *Annals of Botany*, 101(8):1281–1293, 5 2008. ISSN 0305-7364. doi: 10.1093/AOB/MCM199. URL `https://academic.oup.com/aob/article/101/8/1281/160454`.

[19] Peter Davidson. *Turbulence: An Introduction for Scientists and Engineers.* OUP Oxford, 2015.

[20] Jacques Desrues, Edward Andò, Federica A. Mevoli Ando, Laurent Debove, and Gioacchino Viggiani. How does strain localise in standard triaxial tests on sand: Revisiting the mechanism 20 years on. *Mechanics Research Communications*, 92: 142–146, 9 2018. ISSN 00936413. doi: 10.1016/J.MECHRESCOM.2018.08.007.

[21] Stina Drakare and Lars Sonesten. Göta älv - en resa med vattnets kemi från källa till hav, 5 2019.

[22] Hans Albert Einstein and D C Washington. The Bed-Load Function for Sediment Transportation in Open Channel Flows. Technical report, U.S. Department of Agriculture, 1950.

[23] Federal Interagency Stream Restoration Working Group (FISRWG). Stream Corridor Restoration: Principles, Processes and Practices, 1998.

[24] D G Fredlund. Second Canadian Geotechnical Colloquium: Appropriate concepts and technology for unsaturated soils. *Can. Geotech. J.*, 16:121–139, 1979.

[25] Delwyn G. Fredlund and Murray D. Fredlund. Keynote Lecture: Developments in Landslide Analysis. *Lecture Notes in Civil Engineering*, 62:777–794, 2020. ISSN 23662565. doi: 10.1007/978-981-15-2184-3{_}101. URL `https://link.springer.com/chapter/10.1007/978-981-15-2184-3_101`.

[26] Ankit Garg, Anthony Kwan Leung, Charles Wang Wai Ng, and Billy Chi Hang Hau. Effects of Plant Transpiration on Suction Distribution in a Vegetated Soil Slope. *Unsaturated Soils: Research and Applications*, 2:342–357, 2012.

[27] Eleni Gerolymatou, Jelke Dijkstra, and Gunnel Göransson. Towards contemporary erosion solutions. Technical report, Branschsamverkan i grunden, 2020.

[28] Murielle Ghestem, Roy C. Sidle, and Alexia Stokes. The Influence of Plant Root Systems on Subsurface Flow: Implications for Slope Stability. *Bio Science*, 61 (11):869–870, 2011. doi: 10.1525/bio.2011.61.11.6. URL `www.biosciencemag.org`.

[29] Bertil Hallman. Trafikslagsövergripande stråkstudie Göta älv-Vänernstråket. Technical report, Trafikverket, 2016.

[30] Rubin Hillel and Joseph Atkinson. *Environmental Fluid Mechanics*. Marcel Dekker, inc., New York, 2001.

[31] Buddhima Indraratna, Behzad Fatahi, H Khabbaz, Hadi Khabbaz, and B Indraratna. Numerical analysis of matric suction effects of tree roots Numerical analysis of matric suction effects of tree roots Numerical analysis of matric suction effects of tree roots. *Geotechnical Engineering*, 159(GE2):77–90, 2006. URL `https://ro.uow.edu.au/engpapershttps://ro.uow.edu.au/engpapers/395.https://ro.uow.edu.au/engpapers/395`.

[32] Iowa Department of Natural Resources. How to Control Streambank Erosion. Technical report, Iowa Department of Natural Resources, 2006.

[33] Minna Karstunen and Amardeep Amavasai. BEST SOIL: Soft soil modelling and parameter determination. Technical report, Chalmers University of Technology, Gothenburg, 11 2017.

[34] J.A Knappet and R.F Craig. *Craig's Soil Mechanics*. Spoon Press, eighth edition, 2012.

[35] Yong G. Lai, Robert E. Thomas, Yavuz Ozeren, Andrew Simon, Blair P. Greimann, and Kuowei Wu. Modeling of multilayer cohesive bank erosion with a coupled bank stability and mobile-bed model. *Geomorphology*, 243: 116–129, 8 2015. ISSN 0169-555X. doi: 10.1016/J.GEOMORPH.2014.07.017.

[36] Lars-Ove Lång. Beskrivning till kartan Grundvattenförekomster i Göteborgs kommun. Technical report, Sveriges geologiska undersökning, 2009. URL `www.sgu.se`.

[37] Lars-Ove Lång and Bo Thunholm. Geologisk information och modellering i avrinningsområden Slutrapport för FoU-projekt 5273. Technical report, Sveriges Geologiska Undersökning, 2002.

[38] Wei Lanting, Xu Qiang, Wang Shanyong, Wang Cuilin, and Ji Xu. The morphology evolution of the shear band in slope: insights from physical modelling using transparent soil. *Bulletin of Engineering Geology and the Environment*, 79(4):1849–1860, 5 2020. ISSN 14359537. doi: 10.1007/S10064-019-01649-1.

[39] Rolf Larsson. Jords egenskaper - Information 1. Technical report, SGI, Linköping, 2008.

[40] Thoms Ledl. Hannersdorf Tauchenbach.jpg - Wikimedia Commons, 2021. URL `https://commons.wikimedia.org/wiki/File:Hannersdorf_Tauchenbach.jpg`.

[41] S Leroueil. Natural slopes and cuts: movement and failure mechanisms. *Géotechnique*, 51(3):197–243, 2001. doi: https://doi.org/10.1680/geot.2001.51.3.197.

[42] Sape A Miedema. Constructing the Shields curve part C: Cohesion by silt. Technical report, Delft University of Technology, 2013. URL `https://www.researchgate.net/publication/271504462`.

[43] Henning Mohr. *Erosion and scour behaviour of marine sediments*. PhD thesis, The University of Western Australia, 2015.

[44] R. P. C. (Royston Philip Charles) Morgan and R. J. (R. Jane) Rickson. *Slope stabilization and erosion control, a bioengineering approach*. E & FN Spon, 1995. ISBN 0 419 15630 5. URL `https://books.google.com/books/about/Slope_Stabilization_and_Erosion_Control.html?hl=sv&id=q5t5AgAAQBAJ`.

[45] Junaid Munir, Bingheng Liu, Lingwei Kong, Chengsheng Li, and Juntao Wang. Evolution of Shear Band in Plane Strain Compression of Naturally Structured Clay with a High Sensitivity. *Applied Sciences*, 2022. doi: 10.3390/app12031180. URL `https://doi.org/10.3390/app12031180`.

[46] National Geographic Society. The Rock Cycle , 11 2019. URL `https://www.nationalgeographic.org/encyclopedia/rock-cycle/`.

[47] Native wildflowers Nursery. Live stakes, 2022. URL `https://www.nativewildflowers.net/live-stakes/`.

[48] C.W.W Ng, A.K Leung, A. Garg, K.X Woon, L.M Chu, and B.C.H Hau. Soil suction induced by grass and tree in an atmospheric-controlled plant room. In *18th International Conference on Soil Mechanics and Geotechnical Engineering (Paris)*, 2013.

[49] J. J. Ni, A. K. Leung, and C. W.W. Ng. Modelling soil suction changes due to mixed species planting. *Ecological Engineering*, 117:1–17, 7 2018. ISSN 09258574. doi: 10.1016/j.ecoleng.2018.02.023.

[50] Folke Ohlsson, Lars Johansson, Anders Hallingberg, and Marianne Nyberg. EROSIONSSKYDD i samband med förstärkningsåtgärder för slänter. Technical report, IVA Skredkommissionen, Linköping, 1994.

[51] Mats Olsson. Calculating long-term settlement in soft clays - with special focus on the Gothenburg region. Technical report, Chalmers University of Technology, 2010. URL `www.swedgeo.se`.

[52] PARIO. PARIO Meter Manual. Technical report, 2019.

[53] Natasha Pollen and Andrew Simon. Estimating the mechanical effects of riparian vegetation on stream bank stability using a fiber bundle model. *Water resourses reseach*, 41, 2005. doi: 10.1029/2004WR003801.

[54] Bert Reubens, Jean Poesen, Frédéric Danjon, Guy Geudens, and Bart Muys. The role of fine and coarse roots in shallow slope stability and soil erosion control with a focus on root system architecture: A review. *Trees*, 21:385–4002, 2007. doi: 10.1007/s00468-007-0132-4. URL `https://www.researchgate.net/publication/225161719`.

[55] Yannick Y. Rousseau, Marco J. Van de Wiel, and Pascale M. Biron. Simulating bank erosion over an extended natural sinuous river reach using a universal slope stability algorithm coupled with a morphodynamic model. *Geomorphology*, 295: 690–704, 10 2017. ISSN 0169-555X. doi: 10.1016/J.GEOMORPH.2017.08.008.

[56] Bengt Rydell, Karin Lundström, Yvonne Andersson-Sköld, and Per-Evert Bengtsson. Linköping 2012 Slutrapport Del 2 - Kartläggning. Technical report, SGI, 2009. URL `www.swedgeo.se`.

[57] Bengt Rydell, Håkan Persson, Linda Blied, and Wilhelm Rankka. Erosionsförhållanden i Göta älv GÄU -delrapport 1. Technical report, SGI, Linköping, 2011.

[58] J Carlos Santamarina. Soil Behavior and Soft Ground Construction, in honor of Charles C. Technical report, MIT, 2001.

[59] H. Bolton Seed, Richard J. Woodward, and Raymond Lundgren. Fundamental Aspects of the Atterberg Limits. *Journal of the Soil Mechanics and Foundations Division*, 90(6):75–106, 11 1964. ISSN 0044-7994. doi: 10.1061/JSFEAQ.0000685.

[60] Albert Shields. Application of similarity principles and turbulence reseach to bed-load movement. Technical report, California Institute of Technology, 1936.

[61] SMHI. Sveriges största vattendrag, 5 2021.

[62] John Southard. *Introduction to Fluid Motions, Sediment Transport and Current-Generated Sedimentary Structures.* Massachusetts Institute of Technology, 2006.

[63] Alexia Stokes, Joanne E. Norris, L. P. H. van Beek, Thom Bogaard, Erik Cammeraat, Slobodan B. Mickovski, Anthony Jenner, Antonio Di Iorio, and Thierry Fourcaud. *Slope stability and erosion control: ecotechnological solutions.* Springer Science & Business Media, 2008. ISBN 978-1-4020-6676-4. doi: https://doi.org/10.1007/978-1-4020-6676-4{_}4.

[64] Alexia Stokes, Joanne E. Norris, L. P.H. Van Beek, Thom Bogaard, Erik Cammeraat, Slobodan B. Mickovski, Anthony Jenner, Antonino Di Iorio, and Thierry Fourcaud. How Vegetation Reinforces Soil on Slopes. *Slope Stability and Erosion Control: Ecotechnological Solutions*, pages 65–118, 2008. doi: 10.1007/978-1-4020-6676-4{_}4. URL `https://link.springer.com/chapter/10.1007/978-1-4020-6676-4_4`.

[65] Alexia Stokes, Claire Atger, Anthony Glyn Bengough, Thierry Fourcaud, and Roy C. Sidle. Desirable plant root traits for protecting natural and engineered slopes against landslides. *Plant and Soil 2009 324:1*, 324(1):1–30, 9 2009. ISSN 1573-5036. doi: 10.1007/S11104-009-0159-Y. URL `https://link.springer.com/article/10.1007/s11104-009-0159-y`.

[66] Alexia Stokes, Grant B. Douglas, Thierry Fourcaud, Filippo Giadrossich, Clayton Gillies, Thomas Hubble, John H. Kim, Kenneth W. Loades, Zhun Mao, Ian R. McIvor, Slobodan B. Mickovski, Stephen Mitchell, Normaniza Osman, Chris Phillips, Jean Poesen, Dave Polster, Federico Preti, Pierre Raymond, Freddy Rey, Massimiliano Schwarz, and Lawrence R. Walker. Ecological mitigation of hillslope instability: Ten key issues facing researchers and practitioners. *Plant and Soil*, 377(1-2):1–23, 3 2014. ISSN 0032079X. doi: 10.1007/S11104-014-2044-6/TABLES/4. URL `https://link.springer.com/article/10.1007/s11104-014-2044-6`.

[67] Sveriges Geologiska Undersökning. SGUs Kartvisare, 2022. URL `https://apps.sgu.se/kartvisare/kartvisare-jordarter-25-100.html`.

[68] Rocky TALCHABHADEL, Kazuyuki OTA, Hajime NAKAGAWA, and Kenji KAWAIKE. THREE-DIMENSIONAL SIMULATION OF FLOW AND SEDIMENT TRANSPORT PROCESSES IN TIDAL BASIN. *Journal of Japan Society of Civil Engineers, Ser. B1 (Hydraulic Engineering)*, 74(4):I_955–I_960, 2018. ISSN 2185-467X. doi: 10.2208/jscejhe.74.i{_}955.

[69] Karl Terzaghi. Mechanism of Landslides. In *Application of Geology to Engineering Practice*, pages 83–123. Geological Society of America, 4 1950. doi: 10.1130/BERKEY.1950.83.

[70] treesftf. Vetiver Grass in Ethiopia, 2008.

[71] United States Department of Agriculture Natural Resources Conservation Service. Chapter 16 Streambank and Shoreline Protection Engineering Field Handbook. In *Streambank and Shoreline Protection*, volume 650. United States-Department of Agriculture, 1996.

[72] Vägverket. Erosionsskydd i vatten vid väg och brobyggnad. Technical report, Vägverket, 1987.

[73] Rens Van Beek, Erik Cammeraat, Vicente Andreu, Slobodan B. Mickovski, and Luuk Dorren. Hillslope processes: Mass wasting, slope stability and erosion. In *Slope Stability and Erosion Control: Ecotechnological Solutions*, pages 17–64. Springer Netherlands, 2008. ISBN 9781402066757. doi: 10.1007/978-1-4020-6676-4{_}3. URL `https://www.researchgate.net/publication/241004756_Hillslope_Processes_Mass_Wasting_Slope_Stability_and_Erosion`.

[74] M. Th. van Genuchten. A Closed-form Equation for Predicting the Hydraulic Conductivity of Unsaturated Soils. *Soil Science Society of America Journal*, 44(5):892–898, 9 1980. ISSN 1435-0661. doi: 10.2136/SSSAJ1980.03615995004400050002X. URL

https://onlinelibrary.wiley.com/doi/full/10.2136/sssaj1980.03615995004400050002xhttps://onlinelibrary.wiley.com/doi/abs/10.2136/sssaj1980.03615995004400050002xhttps://acsess.onlinelibrary.wiley.com/doi/10.2136/sssaj1980.03615995004400050002x.

[75] Leo Van Rijn. Sediment pick-up functions. *Journal of Hydraulic Engineering ASCE*, 10, 1984.

[76] Leo Van Rijn. Sediment Transport, Part I: Bed load transport. *Journal of Hydraulic Engineering ASCE*, 10, 1984.

[77] Leo Van Rijn. Sediment Transport, Part II: Suspended load transport. *Journal of Hydraulic Engineering ASCE*, 11, 1984.

[78] Leo van Rijn. Simple general formulae for sand and transport in rivers, estuaries and costal waters. *Retrieved from www. leovanrijn-sediment. com*, 2013. URL www.leovanrijn-sediment.com.

[79] I. Vardoulakis. Shear band inclination and shear modulus of sand in biaxial tests. *International Journal for Numerical and Analytical Methods in Geomechanics*, 4(2):103–119, 4 1980. ISSN 1096-9853. doi: 10.1002/NAG.1610040202. URL https://onlinelibrary.wiley.com/doi/full/10.1002/nag.1610040202https://onlinelibrary.wiley.com/doi/abs/10.1002/nag.1610040202https://onlinelibrary.wiley.com/doi/10.1002/nag.1610040202.

[80] Västkuststiftelsen. Göta och Nordre älvs dalgång, 2022. URL https://www.lansstyrelsen.se/vastra-gotaland/besoksmal/naturreservat/gota-och-nordre-alvs-dalgang.html.

[81] L. J. Waldron. The Shear Resistance of Root-Permeated Homogeneous and Stratified Soil. *Soil Science Society of America Journal*, 41(5):843–849, 9 1977. ISSN 1435-0661. doi: 10.2136/SSSAJ1977.03615995004100050005X. URL https://onlinelibrary.wiley.com/doi/full/10.2136/sssaj1977.03615995004100050005xhttps://onlinelibrary.wiley.com/doi/abs/10.2136/sssaj1977.03615995004100050005xhttps://acsess.onlinelibrary.wiley.com/doi/10.2136/sssaj1977.03615995004100050005x.

[82] Willow. File:Salix alba 004.jpg - Wikimedia Commons, 4 2007. URL https://commons.wikimedia.org/wiki/File:Salix_alba_004.jpg.

[83] Muir Wood, Anthony Glyn, G J Meijer, D Muir Wood, J A Knappett, A G Bengough, and T Liang. Root reinforcement: continuum framework for constitutive modelling. *Geotechnique*, 2022. doi: 10.1680/jgeot.21.00132. URL https://doi.org/10.1680/jgeot.21.00132.

[84] Tien H. Wu, William P. McKinnell, and Douglas N. Swanston. Strength of tree roots and landslides on Prince of Wales Island, Alaska. *Canadian Geotechnical Journal*, 16(1):19–33, 1979. ISSN 00083674. doi: 10.1139/T79-003. URL https://cdnsciencepub.com/doi/abs/10.1139/t79-003.

[85] H. Zhu and Limin M. Zhang. Evaluating suction profile in a vegetated slope considering uncertainty in transpiration. *Computers and Geotechnics*, 63:112–120, 1 2015. ISSN 18737633. doi: 10.1016/j.compgeo.2014.09.003.

[86] H. Zhu, L. M. Zhang, and A. Garg. Investigating plant transpiration-induced soil suction affected by root morphology and root depth. *Computers and Geotechnics*, 103:26–31, 11 2018. ISSN 0266-352X. doi: 10.1016/J.COMPGEO.2018.06.019.

A

Historical photos of case study sites

Figure A.1: Oxhagen, present day aerial photo. The approximate location of the shoreline in year 1960 is marked with dark red dots and the approximate location of the case study area is marked with red rectangle.

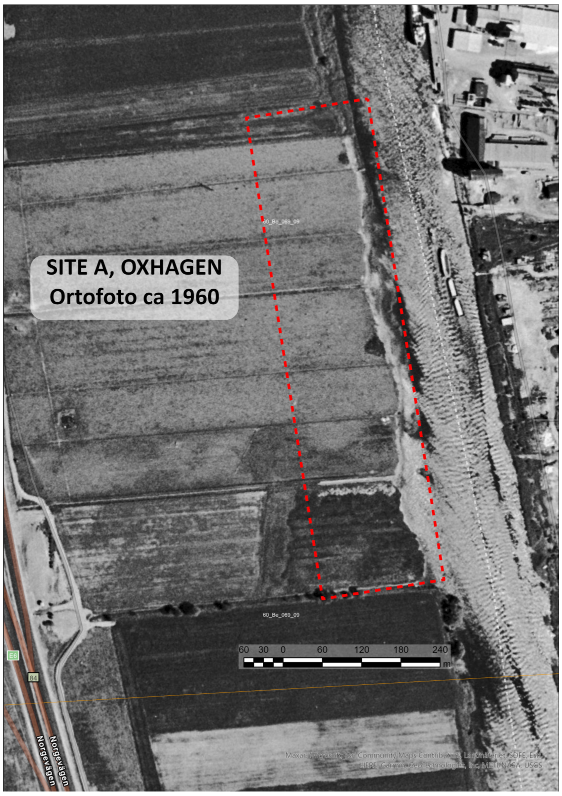

Figure A.2: Oxhagen year 1960

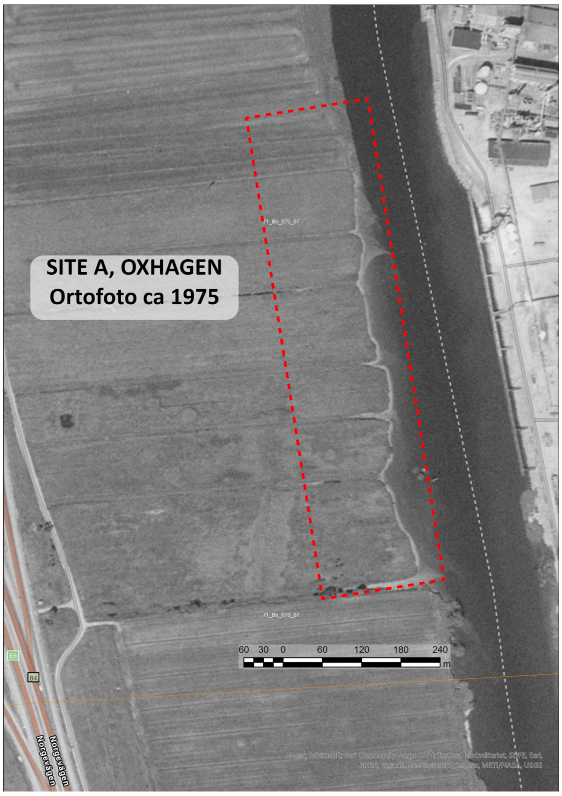

Figure A.3: Oxhagen year 1975

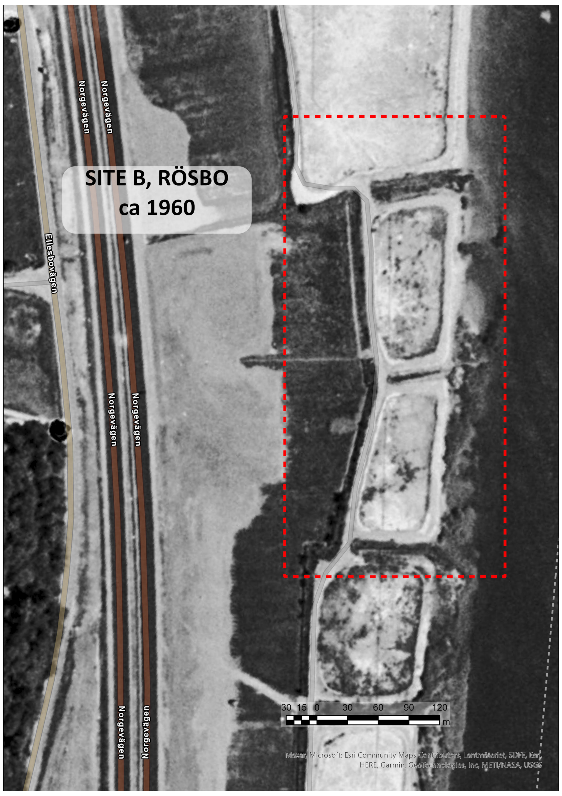

Figure A.4: Rösbo year 1960

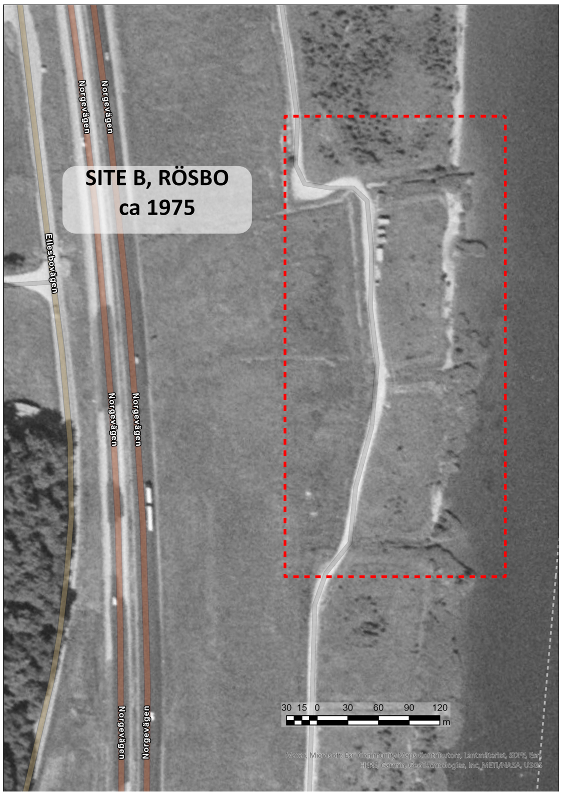

Figure A.5: Rösbo year 1975

Figure A.6: Rösbo present day photo. The approximated location of the shoreline in year 1960 is marked with red dots

B

Pictures from site visit

Pictures of site visits at case study sites and sampling.

Figure B.1: Soil sampling 20220225.

Figure B.2: NBS type B2 at low water level, 20220126.

Figure B.3: NBS type B2 during a high water level 2022-02-25.

C

Results from laboratory work, particle size distribution

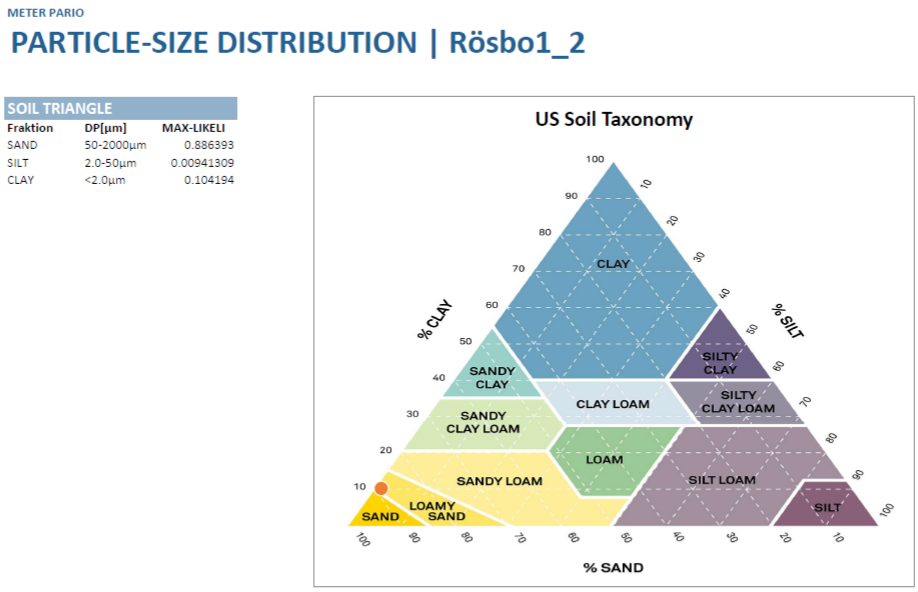

Figure C.1: Particle size distribution for Rösbo 1.2, loamy sand.

METER PARIO

PARTICLE-SIZE DISTRIBUTION | Rösbo2_2

SOIL TRIANGLE		
Fraktion	DP[µm]	MAX-LIKELI
SAND	50-2000µm	0.743834
SILT	2.0-50µm	0.177613
CLAY	<2.0µm	0.0785521

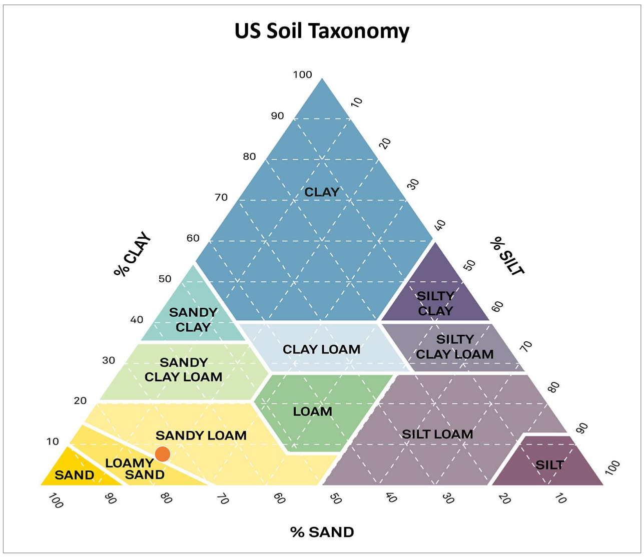

Figure C.2: Particle size distribution for Rösbo 2.2, sandy loam.

METER PARIO

PARTICLE-SIZE DISTRIBUTION | Rösbo3a

SOIL TRIANGLE		
Fraktion	DP[µm]	MAX-LIKELI
SAND	50-2000µm	0.850436
SILT	2.0-50µm	0.0147891
CLAY	<2.0µm	0.134775

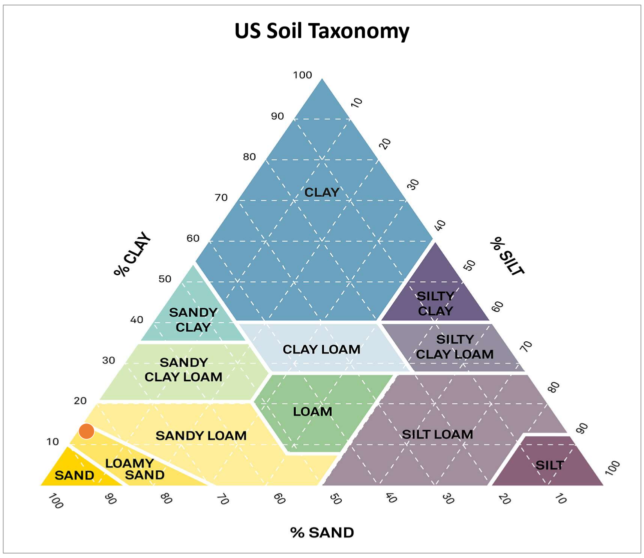

Figure C.3: Particle size distribution for Rösbo sample 3a, loamy sand.

METER PARIO

PARTICLE-SIZE DISTRIBUTION | Rösbo_3b

SOIL TRIANGLE		
Fraktion	**DP[µm]**	**MAX-LIKELI**
SAND	50-2000µm	0.286603
SILT	2.0-50µm	0.407671
CLAY	<2.0µm	0.305725

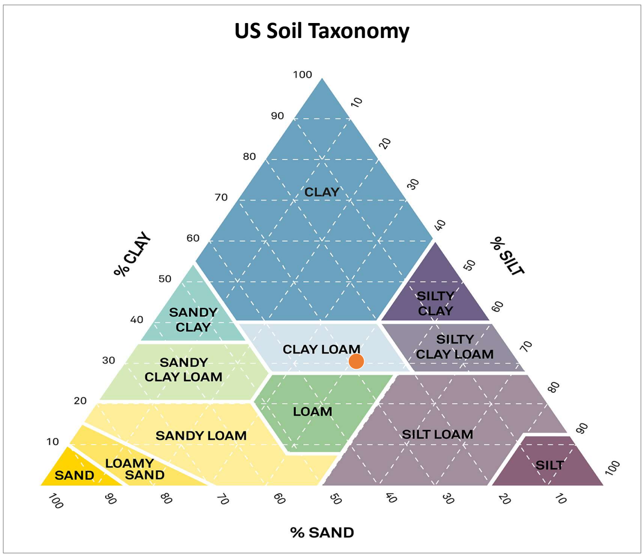

Figure C.4: Particle size distribution for Rösbo 3b, clay loam.

D

Soil test tool in Plaxis

This appendix include the result from the soil test tool in Plaxis that are used to verify the input parameters that are approximated through empirical relationships.

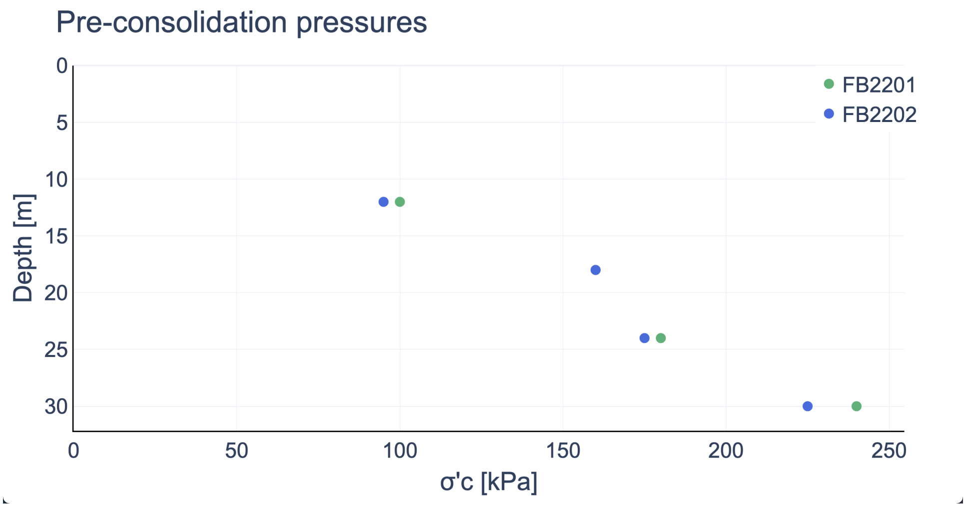

Figure D.1: Pre-consolidation pressure from CRS.

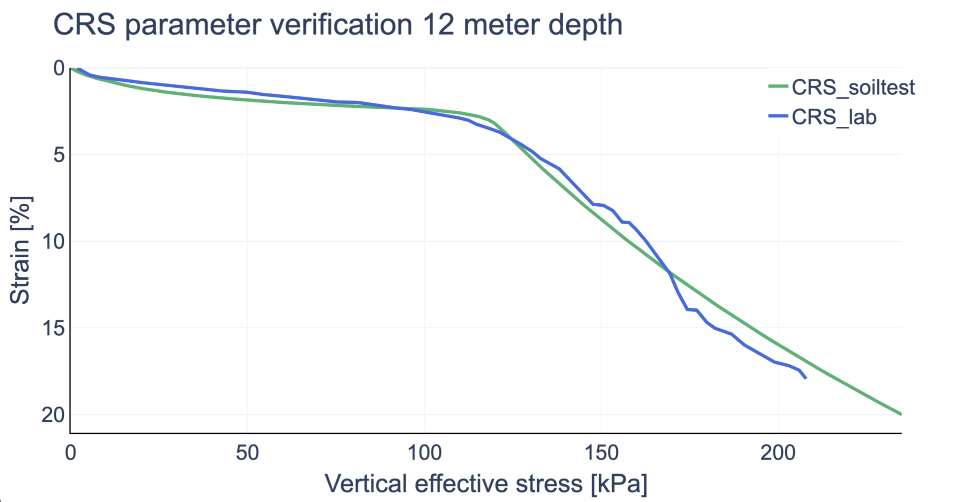

Figure D.2: Parameter verification CRS test at 12 meter depth.

E

Mesh

This appendix include an extract from the final mesh quality in used in the Plaxis 2D model. The mesh of the slope is shown but not the complete model as it is the mesh of the slope will be the most relevant for the result.

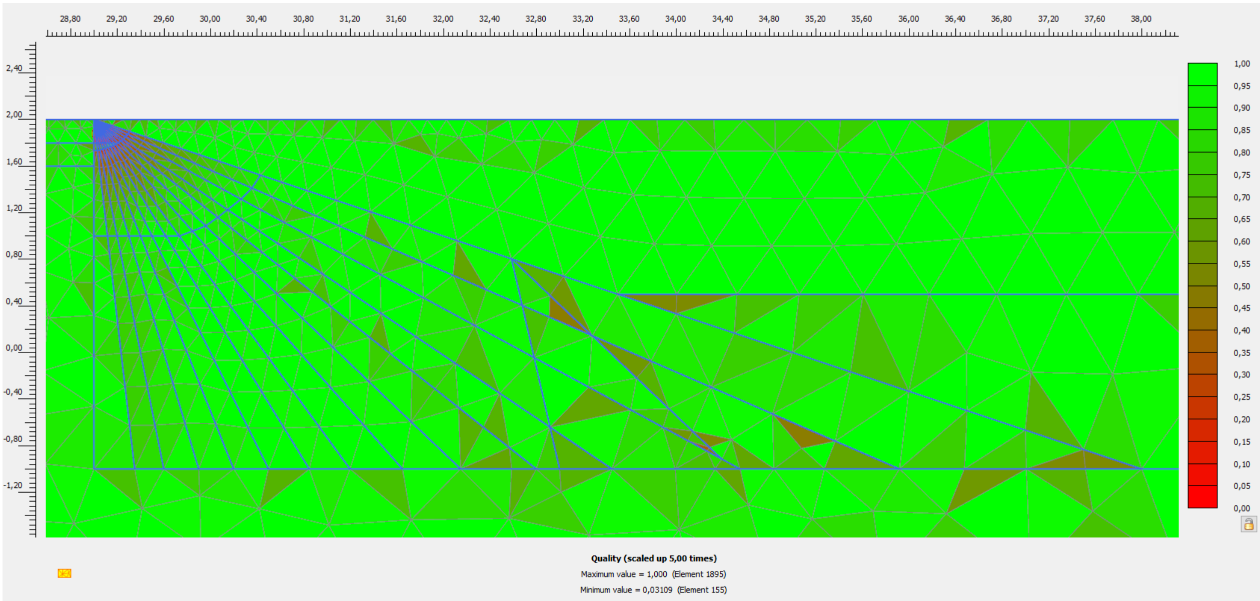

Figure E.1: Final mesh quality used in the Plaxis analysis.

F

Results from the numerical analysis

Plots of the low, medium and high head boundary slopes for angles after which the bare slope has failed. The low boundary slope fails after 48.43°, the medium and high boundary slopes do not fail at 63.43° which is the steepest angle tested.

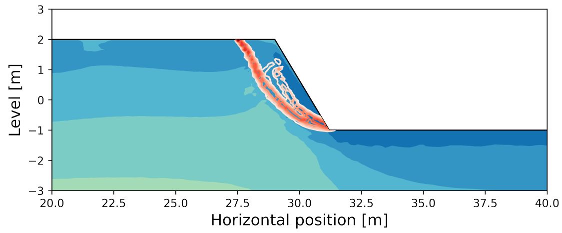

(a) Low head boundary

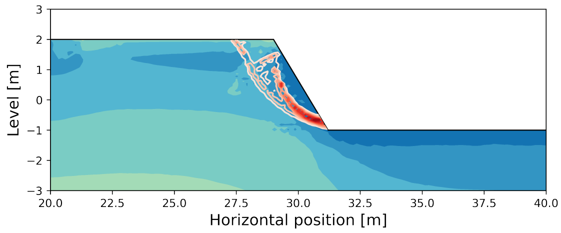

(b) Medium head boundary

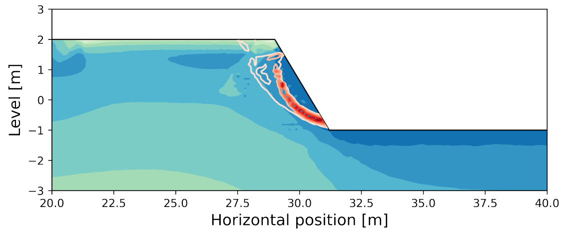

(c) High head boundary

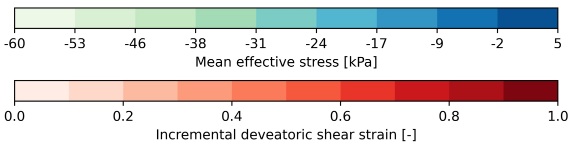

(d) Colorbar for contour plots

Figure F.1: Slope angle 53.43°

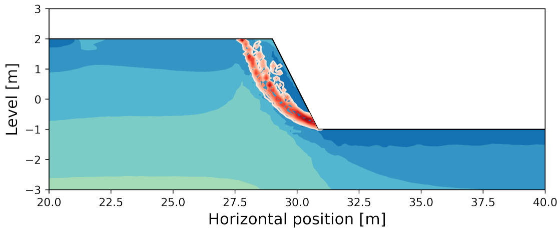

(a) Low head boundary

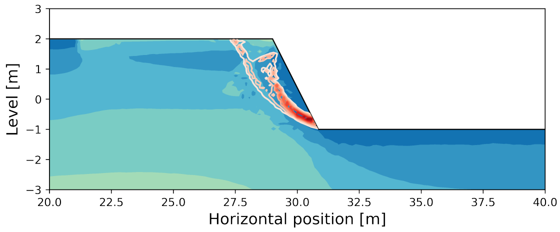

(b) Medium head boundary

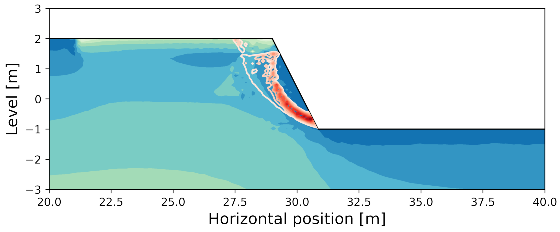

(c) High head boundary

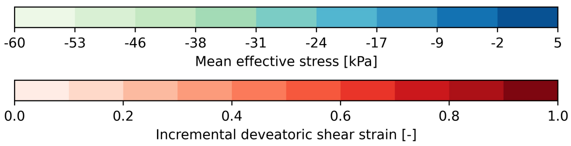

(d) Colorbar for contour plots

Figure F.2: Slope angle 58.43°

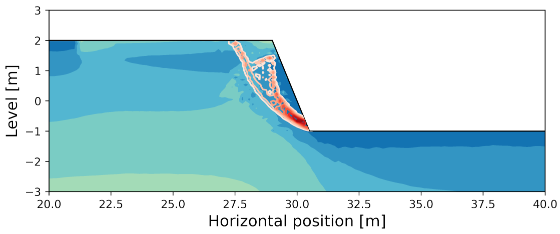

(a) Medium head boundary

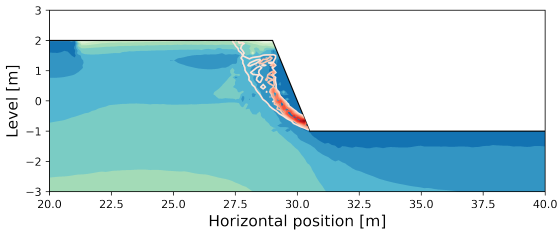

(b) High head boundary

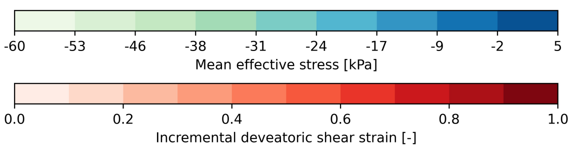

(c) Colorbar for contour plots

Figure F.3: Slope angle 58.43°

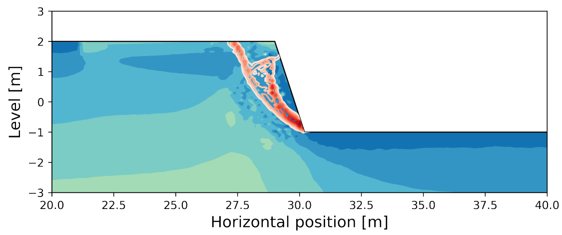

(a) Medium head boundary

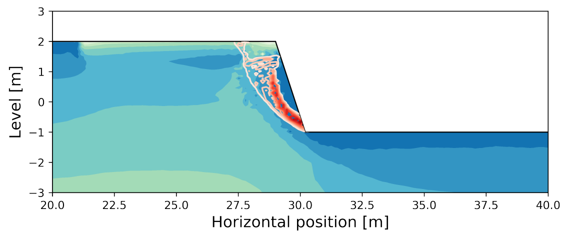

(b) High head boundary

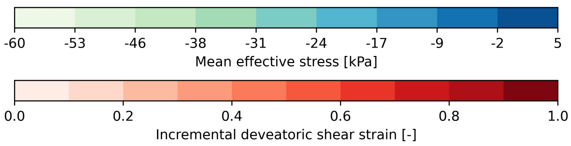

(c) Colorbar for contour plots

Figure F.4: Slope angle 63.43°

DEPARTMENT OF ARCHITECTURE AND CIVIL ENGINEERING
CHALMERS UNIVERSITY OF TECHNOLOGY
Gothenburg, Sweden
www.chalmers.se

CHALMERS
UNIVERSITY OF TECHNOLOGY